**Establishing the biological role of MPK20 in primary cell wall formation in *Arabidopsis***

**by**

**Siyu Cheng**

**A THESIS SUBMITTED IN PARTIAL FULFILLMENT OF**

**THE REQUIREMENTS FOR THE DEGREE OF**

**MASTER OF SCIENCE**

**in**

**THE FACULTY OF GRADUATE AND POSTDOCTORAL STUDIES**

**(Land and Food Systems)**

**THE UNIVERSITY OF BRITISH COLUMBIA**

**(Vancouver)**

**May 2015**

## Abstract

Plants, as sessile organisms, need to grow while withstanding many environmental challenges. To give this capability, various cellular signal transduction systems are necessary for sensing changes in the environment and transmitting these signals to other components of the cell. One of the major mechanisms used for such signal transmission consists of mitogen-activated protein kinase (MAPK) cascades.

MAPK cascades form an important signal transduction system in all eukaryotic organisms. In *Arabidopsis thaliana*, 20 MAPKs (MPKs) have been found, which belong to two sub-types: the TEY sub-type (MPK Groups A, B, and C) and the TDY sub-type (MPK Group D). Very little is known about the biological roles of Group D MPKs, but the expression of one group D MPK, MPK20, is correlated across many microarray experiments with expression of primary cell wall cellulose synthase (CesA) genes – CesA1, 3, and 6 [1]. This suggests that MPK20 may be involved in primary cell wall synthesis or associated biochemical processes. According to data in the MIND 0.5 database (Membrane-protein Interaction Network Database 0.5), MPK20 interacts with AtPIN1. As auxin is important for cell wall loosening and cell expansion, such an association with an auxin transporter could indicate that MPK20 plays a role in auxin signaling pathways, especially those that affect cell walls.

In this study, the biological function of MPK20 has been explored by reverse genetics and phenotype assays. The *mpk20 knock out* (*KO*) lines display shorter hypocotyls and shorter primary roots compared with wild type (WT). However, these growth differences are small, although statistically significant. As MPK18, MPK19 and MPK20 are close homologues, double and triple KO mutants were built and analyzed. The loss-of-function mutants do not display any detectable auxin-related phenotype, nor do they differ from WT plants with respect to responses to other plant hormones tested except in their response to exogenous GA application. Attempts were made to purify a recombinant protein of MPK20 but these were unsuccessful. To explain the results of these experiments, models of MPK20 biological function, and of its interactions with the MPK20 paralogues, MPK18 and MPK19, have been proposed.

## Preface

This dissertation is original, unpublished, independent work by the author, S. Cheng

## Table of Contents

## List of Tables

## List of Figures

## List of Abbreviations

| | |
|---|---|
| MAPK, MPK | mitogen-activated protein kinase |
| MIND 0.5 database | membrane-protein interaction network database 0.5 |
| mbSUS system | mating-based split ubiquitin system |
| *KO* | knock-out |
| PCR | polymerase chain reaction |
| SQ RT-PCR | semi-quantitative reverse-transcription PCR |
| GUS | β -glucuronidase |
| MAPKKK | MPK kinase kinase |
| MAPKK, MEK, MKK | MPK kinase |
| PK | protein kinase |
| NRL | neural retina leucine (a human basic motif-leucine zipper protein transcription factor) |
| MAP2 kinase | microtubule-associated protein-2 kinase |
| ANP | *Arabidopsis* NPK1-like protein kinase |
| ETR1 | Ethylene-Resistant 1 |
| CTR1 | Constitutive Triple-Response 1 |

| | |
|---|---|
| NTF2 | Nuclear Transport Factor 2 |
| MKP | MAP kinase phosphatase |
| SAPK | stress-activated protein kinase |
| JNK | c-jun N-terminal kinase |
| PAT | polar auxin transport |
| Y2H | yeast two-hybrid |
| JA | jasmonic acid |
| SA | salicylic acid |
| qRT-PCR | quantitative real-time PCR |
| ACC | 1-aminocyclopropane-l-carboxylic acid |
| CSC | cellulose synthase complex |
| SNPs | single nucleotide polymorphisms |
| MS | Murashige and Skoog |
| TAE | Tris-Acetate-EDTA |
| RT | room temperature |
| DEPC | diethylpyrocarbonate |
| SDS-PAGE | sodium dodecyl sulfate - polyacrylamide gel electrophoresis |
| TEMED | tetramethylethylenediamine |

| | |
|---|---|
| PVDF | polyvinylidene difluoride |
| BRZ | brassinazole |
| DMSO | dimethyl sulfoxide |
| GA | gibberellic acid |
| PAC | paclobutrazol |
| PTG | isopropyl β-D-1-thiogalactopyranoside |

## Acknowledgements

First of all, I owe my deepest gratitude to my supervisor, Dr. Brian Ellis. I would like to thank him for the endless support of my study and this program, for his motivation, enthusiasm, and immense knowledge. His guidance helped me in all the time of research and writing of this thesis.

My sincere thanks also goes to my co-supervisor Dr. Geoffrey Wasteneys and committee member Dr. Jim Kronstad for their time to review my thesis and scientific advice to this project.

I thank the lab members, Dr. Albert Cairo, Dr. Mathias Schuetz, Dr. Rebecca Smith, Dr. Hardy Hall, and Dr. Zhenhua Yong, for the inspiriting discussions, for the experiments we were working together, and for all the fun we had in the past few years. I would also like to thank the WOW (Working on Walls) program which I learned a lot from.

I cannot find words to express my gratitude to my parents, Xiaojiu Cheng and Fang Guo. This thesis is dedicated to them.

# 1 Introduction

Plants, as sessile organisms, have evolved the capacity to grow and reproduce in the face of many environmental challenges, ranging from UV irradiation, drought and extreme temperature to attacks by herbivores and microbial pathogens. Long-term reproductive success thus depends on a plant's ability to constantly monitor its environment, to integrate these inputs and use them to assess the potential impact of environmental changes, and finally to mobilize appropriate cellular and tissue responses. This requirement has led to the evolution of complex signal detecting and processing systems that connect perceived environmental cues to fine-tuned changes in metabolism, protein activity and transcriptional programming. These signal transduction systems involve an array of mediators, including ion fluxes, phytohormone levels, and post-translational protein modifications, such as mitogen-activated protein kinase (MAPK) cascades.

In plants, MAPK cascades are best known for their involvement in responses to endogenous and environmental signals. Signaling through some MAPK cascades can be triggered by endogenous stimuli such as plant hormones, and/or by external stress stimuli such as temperature extremes, drought, changes in osmotic pressure, pathogen infection, wounding, and ozone challenge. The canonical MAPK cascade module involves members of three PK families: MPK kinase kinases (MAPKKKs), MPK kinases (MAPKKs, MEKs, MKKs) and MAPKs (MPKs). However, none of these signaling response pathways has been completely characterized in plants, and only a small number of kinases within these three MAPK cascade families have been well studied.

## 1.1 Protein phosphorylation/dephosphorylation

Protein phosphorylation catalyzed by protein kinases (PKs) is a particularly important mechanism for rapidly altering protein functionality. Addition of one or more phospho-groups to a given protein has the potential to alter its stability, catalytic activity, sub-cellular location, and/or interactions with other proteins, and these phosphorylation-driven changes can influence a wide range of downstream processes. In the event that the initial trigger for such a protein phosphorylation event is the detection of an environmental change, these kinase-catalyzed

change(s) link detection of the cue with cellular responses, and thus define a signal transduction pathway. In addition, since an activated PK acts catalytically, it can rapidly phosphorylate many target molecules, thereby amplifying the initial signal. In many cases, the activated kinase may also phosphorylate a range of targets simultaneously, which allows the transduced signal to be channeled to multiple downstream outputs.

Given the versatility of protein phosphorylation as a mechanism for transmitting signaling information, it is not surprising that an estimated 40-50% of cellular eukaryotic proteins are predicted to exist in at least one phosphorylated isoform at some point in their lifetime [2-4]. The phosphorylated isoform is believed to have a specific function, distinct from the unphosphorylated form, and it is typically expected to be expressed differently during development, compared with the original protein. Some proteins even have multiple phosphorylated isoforms. For instance, in mammalian retina, NRL (Neural Retina Leucine) can be phosphorylated to as many as six different isoforms [5]. These distinct isoforms may be produced by one or multiple PKs. Enzymes are usually highly specific for their substrates, but the majority of PKs tested appear to be able to phosphorylate multiple different substrates. This could explain why the variety of PKs in the cell is much lower than that of predicted phosphorylated protein isoforms. This catalytic promiscuity and network complexity also greatly increases the difficulty for us to identify each pathway in which specific PKs might be involved.

## 1.2 The biological function of AtMAPKs

### 1.2.1 MPKs in Arabidopsis

Within the PK super-family, the members of the highly conserved MAPK cascades have been intensively studied in many eukaryotic organisms, particularly mammals, yeast and nematodes. MICROTUBULE ASSOCIATED PROTEIN-2 (MAP2) KINASE was the first MAPK to be identified. It was isolated and characterized from animal cells in 1986 [6]. Since that time, many more MAPKs have been characterized, and found to contribute to processes such as nerve growth,

osmotic stress responses, cell division, epidermal cell growth and other physiological, developmental and hormonal responses in animals, yeast and plants.

Although the structures of these kinases are highly conserved among species, their functions vary significantly. Plant genomes are particularly rich in PKs of various classes; indeed, approximately 3% of the *Arabidopsis thaliana* genome is estimated to encode members of the PK super-family. In plants, members of putative MAPK cascades seem to be involved in the responses to biotic and abiotic stress signaling (pathogen infection, drought, salinity, ozone), intracellular signaling of plant hormones, and wound signaling [7]. However, none of these signaling pathways has been completely characterized, and only a subset of the *Arabidopsis* MAPKKKs, MKKs and MPKs have been identified so far as potential players.

MAPKKKs represent the first signaling PK gene family in the cascade. MAPKKKs activate MKKs by phosphorylating the conserved serine and/or threonine residues in their activation loop (T-loop). According to previous studies, the genome of *Arabidopsis* encodes over 60 MAPKKKs [7], and their primary structures are more varied than the structures of MPKs or MKKs. Plant MAPKKKs can be separated into three groups, and each group can be further categorized into a few subgroups. Group A MAPKKKs share the typical kinase domain of classical mammalian MAPKKKs, while Group B and Group C MAPKKKs are more closely related to the human PK, RAF kinase. As these RAF-like MAPKKKs in plants have not been characterized biochemically, the nomenclature of plant MAPKKKs has not been decided yet, and the accurate membership of the AtMAPKKK gene family still needs to be fully determined.

Several studies have found that various AtMAPKKKs are responsive to stresses. For example, *Arabidopsis* NPK1-like protein kinases (ANPs) participate in a $H_2O_2$-responsive signaling pathway [8]; the expression of *AtMAPKKK1* is increased when the plant is treated with cold, salt stress or touch [9]; and EThylene-Resistant 1 (ETR1) and Constitutive Triple-Response 1 (CTR1) kinases are involved in ethylene signaling pathways [10].

MKKs provide the linkage between MPKs and MAPKKKs in the cascade. Generally, MAPKKKs can only phosphorylate MKKs, rather than directly phosphorylating a MPK, although there is at least one exception to this rule. It has been reported that MPK4 interacts

physically with MEKK1, and can be activated by MEKK1 in protoplasts after $H_2O_2$ treatment [11, 12]. In addition, MPK4 interacts with MEKK2 in Y2H assays, and it also phosphorylated by recombinant MEKK2 *in vitro* [13]. Generally, however, MKKs are considered essential for passing the signal from MAPKKKs towards MPKs.

Twenty-one plant MKKs have been identified experimentally, including ten encoded in the *Arabidopsis* genome [7], and almost all possess a conserved S/TxxxS/T phosphorylation target sequence. The exception appears to be AtMKK10, which does not have three amino acids between the two S/T phosphorylation sites. The N-terminal extension of plant MKK proteins typically contains a cluster of basic [K/R] residues N-terminal to a hydrophobic [L/I] site, and this is part of the putative 'MPK docking site' that is thought to mediate the physical interaction of MKKs with their MPK substrates.

Based on amino acid sequence alignment, the MKK gene family has been classified into four groups (A-D) [7]. Group A and Group C MKKs seem to be primarily associated with stress-response pathways. For example, in Group A, MKK2 is activated by stress stimuli such as bacterial elicitor, cold and high salinity [14-16]. In Group C, MKK4 and MKK5 show similar responsiveness towards abiotic stress, but also mediate biotic stress responses such as pathogen challenge and ROS accumulation [17, 18].

The MKKs of Group B have somewhat unusual structures compared with other MKK groups, in that there is a Nuclear Transport Factor 2 (NTF2)-like domain in the C-terminal extension. Among the Group D MKKs, MKK7 seems to help regulate polar auxin transport [19], while MKK9 was found to be involved in regulation of seedling stress tolerance and phytoalexin accumulation in *Arabidopsis* [20]. However, the biological roles of some MKKs, notably MKK8 and MKK10, are still essentially unknown.

The MPKs are the terminal PKs in MAPK cascades. MPKs are phosphorylated by MKKs and dephosphorylated by MAP kinase phosphatases (MKPs). Interestingly, all plant MPKs belong to the mammalian ERK subfamily of MAPKs (Figure 1.1), and no homologues of the other classes of mammalian stress-activated protein kinases (SAPKs), such as c-jun N-terminal kinase (JNK) or p38 kinase, have been detected in plant genomes.

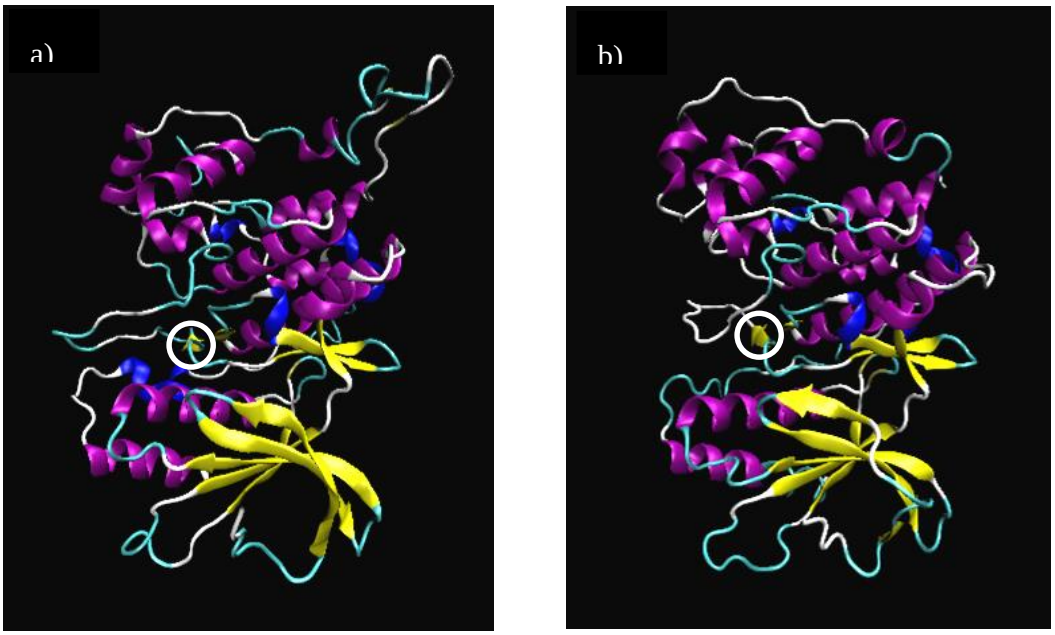


**Figure 1.1: 3D protein structure of ERK1-a and AtMPK6.**

a) ERK1-a protein structure [21]

b) AtMPK6 protein structure simulation by SWISS-MODEL [22-25]

The white circle shows the position of the TEY motif.

### 1.2.2 Group A-C MPKs

All MAPK proteins have in common eleven subdomains characteristic for serine/threonine protein kinases. As a general rule, MPKs are activated by dual phosphorylation of specific Thr and Tyr residues in a TxY motif located in the MPK catalytic activation loop near the 8$^{th}$ domain (Figure 1.3 & 1.4). Based on amino acid sequence alignment, plant MPKs can be defined as belonging to four groups, among which two subtypes are found: the TEY subtype and the TDY subtype. Groups A, B and C have a TEY motif at the phosphorylation site, while Group D MPKs have a TDY motif.

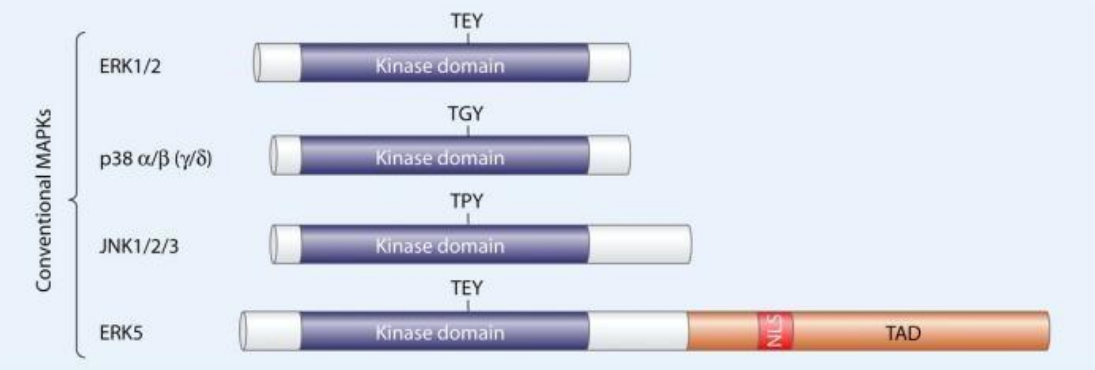


**Figure 1.2: Schematic representation of the human MPKs protein domains.**

These MPKs all have kinase domains, which contain different TxY motifs. TAD represents the transactivation domain; NLS represents the nuclear localization sequence [26].

A few of the 20 MPKs in *Arabidopsis* have been studied intensively, but the functions of most of the others are not well understood. MPK3 and MPK6 are both members of the plant Group A MPKs and their biological functions are at least partially redundant. It has been reported that these two MPKs are involved in various biological processes, such as pathogen defense, abiotic stress-induced responses and stomatal development [17, 27-35]. Another Group A MPK, AtMPK10, has been found to physically interact with AtMKK2. In addition, the cotyledons of *mpk10* and *mkk2 ko* mutants have reduced vein complexity, a phenotype that can be reversed through application of a polar auxin transport (PAT) inhibitor. This suggests that AtMPK10 might be involved in control of venation development by influencing PAT efficiency [36].

The most extensively studied MPK in Group B MPKs is MPK4. This MPK has been reported to be involved in regulating cold, drought and salt resistance [35, 37-42], microtubule bundling in cytokinesis [43, 44], and pathogen resistance [13, 14, 45-47]. AtMPK11 is a close paralogue of MPK4; it interacts with AtMKK6 in yeast two-hybrid (Y2H) assays [42, 48] and has been reported to be involved in pathogen defense and perhaps embryo or seed development, both functions of which MPK4 is also involved [49]. AtMPK12 is localized in guard cells and regulates stomatal closure in response to ABA and $H_2O_2$ treatment [50, 51]. AtMPK5 activates WRKY 62, whose expression is induced by jasmonic acid (JA) and salicylic acid (SA) treatment

[52, 53]. Finally, AtMPK13, which also interacts with AtMKK6, is involved in lateral root formation [42].

There is not much information published about the functions of Group C MPKs. The activities of AtMPK1 and AtMPK2 have been found to be up-regulated in response to wounding, JA, ABA, and $H_2O_2$ stress [7]. AtMPK7 and AtMPK14 were not phosphorylated by any AtMKKs *in viv*o (*Nicotiana benthamiana* leaves) [54], but GhMPK7 (a group C MPK homologue in *Gossypium hirsutum*) has been reported to be involved in a SA-regulated pathogen resistance pathway [55].

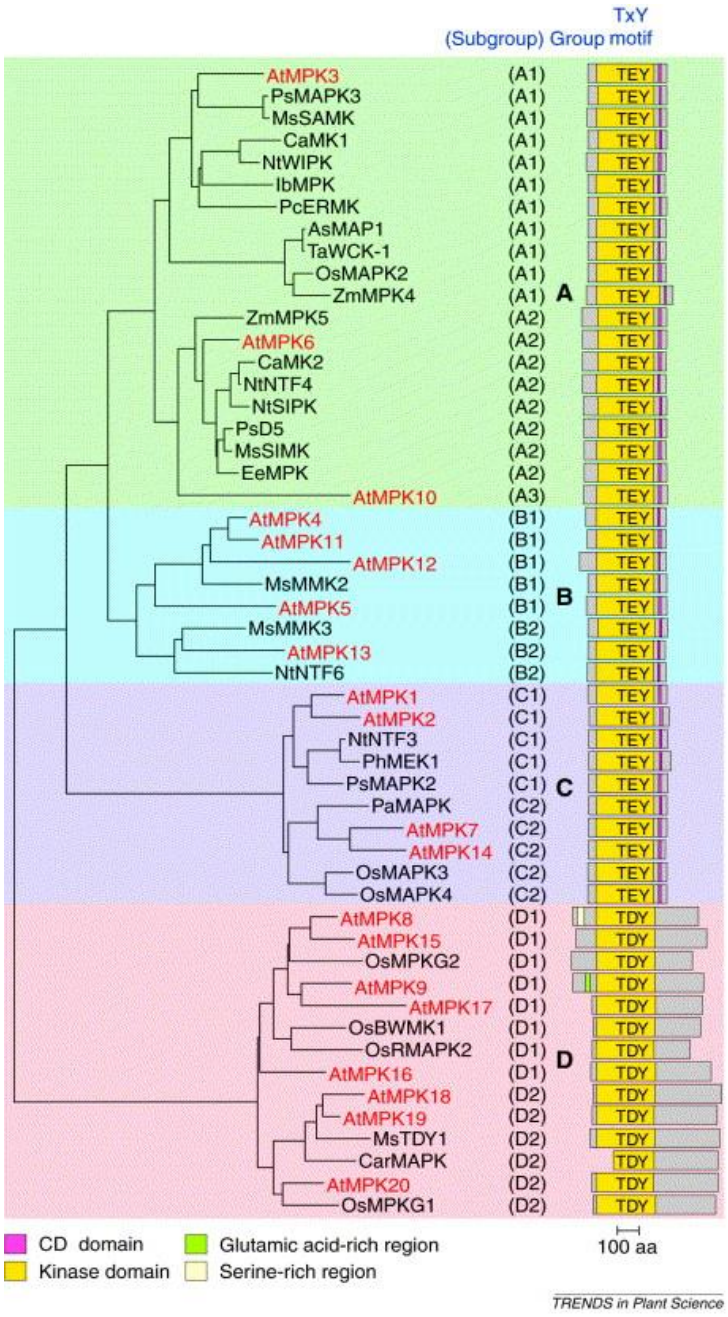


**Figure 1.3: Phylogenetic tree of plant MPKs [7].**

The red letters are *Arabidopsis* MPKs. Other species acronym before the protein name: As, *Avena sativa*; At, *Arabidopsis thaliana*; Ca, *Capsicum annuum*; Car, *Cicer arietinum*; Ee, *Euphorbia esula*; Ib, *Ipomoea batatas*; Ms, *Medicago sativa*; Nt, *Nicotiana tabacum*; Os, *Oryza sativa*; Pa, *prunus armeniaca*.

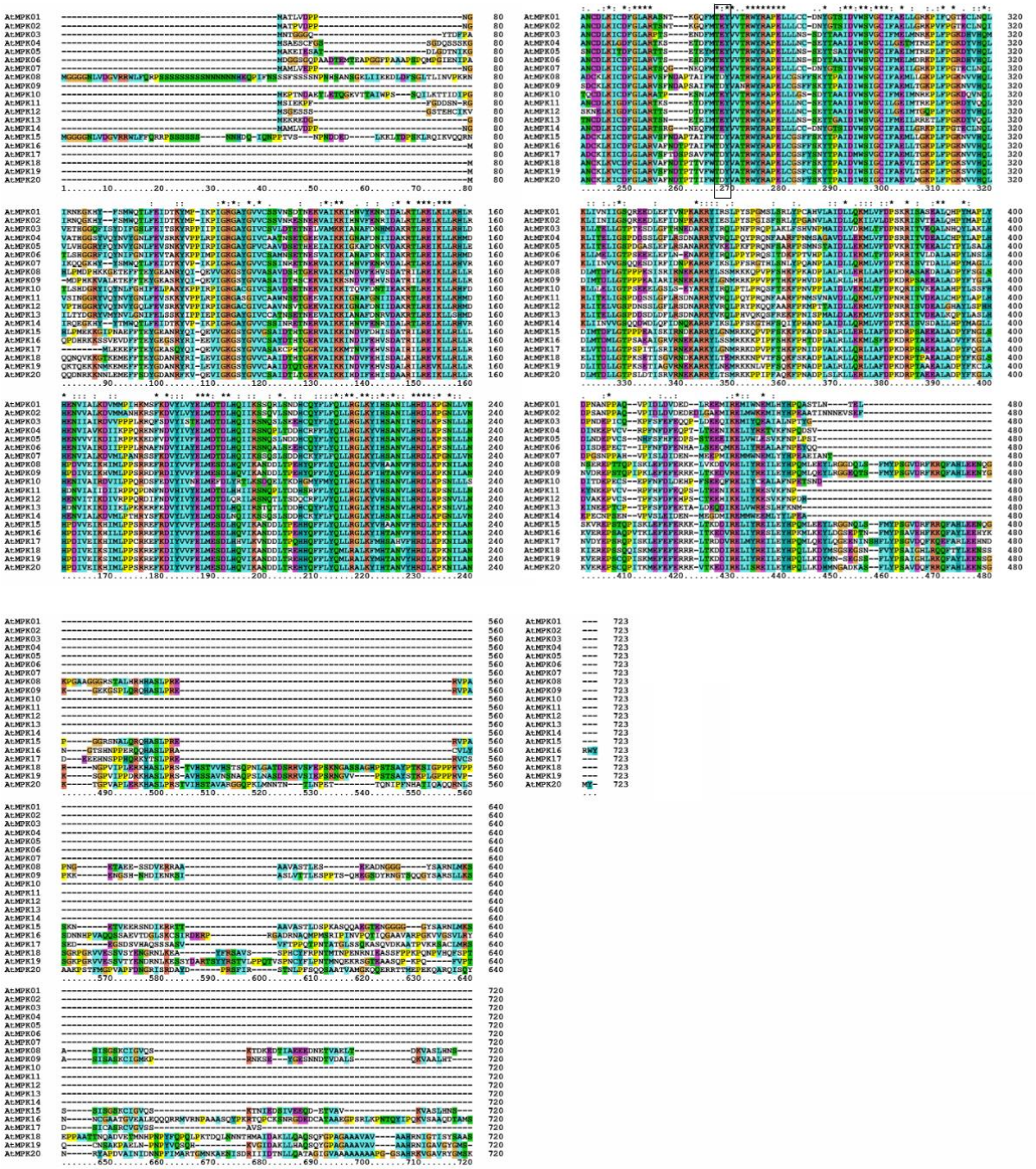

**Figure 1.4: Alignment of the twenty Arabidopsis MPK protein sequences in Clustal X.**

The black box shows the location of the TxY motif. The background of Clustal X sees appendix 1.

### 1.2.3 Group D MPKs

The Group D AtMPKs, consisting of MPK8, 9, 15, 16, 17, 18, 19 and 20, possess unique structural features, including a -TDY- phosphorylation site, instead of -TEY-, and extended N- and C- termini. Very little is known about the biological roles of the Group D MPKs.

In rice, the expression of *OsMPK12* (*OsBWMK1*) transcripts is increased by wounding and by fungal infection [56], while the expression of *OsMPK8* (*OsWJUMK1*) is increased by treatment with heavy metals or ABA, and by pathogen attack [57]. Within 24h of fungal challenge, expression of *OsMPK7, 12* and *15* transcripts increases. Expression of these three MPKs is also increased by JA treatment. According to quantitative real-time PCR (qRT-PCR) analysis, *OsMPK12* expression is increased by ABA treatment, whereas gene expression of *OsMPK12, 13* and *17* is increased by treatment with the ethylene precursor, 1-aminocyclopropane-l-carboxylic acid (ACC). In addition, expression of *OsMPK12,* and *13* is increased by SA treatment [58].

In alfalfa, the expression pattern of *PrTDY1:GUS* suggests that TDY1 might function in root and nodule development, and its expression is also induced in response to wound stress [59]. In tobacco, NTF6 (a putative homolog of AtMPK16) functions in cell division via a proposed NPK1/MEK1/NTF6 cascade [60]. In maize, expression of *ZmMPK17* is influenced by various stresses, as determined by Northern blot analyses, and its C-terminal domain was shown to be essential for its nuclear localization [61]. *GhMPK16* is the first group D MAPK gene to be identified in cotton. Ectopic expression of a *GhMPK16-GFP* construct showed that GhMPK16 is likely localized to the nucleus. Various abiotic and biotic stresses can induce expression of *GhMPK16*, based on the results of an RNA blot assay [55].

### 1.2.4 Previous research on MPK20

Among the Arabidopsis Group D MPKs, MPK20 is of particular interest because its expression is correlated across many microarray experiments with expression of genes involved in primary cell wall biosynthesis, including the "primary cell wall *CesAs*", *CesA 1, 3* and *6* [62]. Since MAPKs post-translationally modify other proteins (enzymes, structural proteins, transcription

factors, etc.), this observation implies that MPK20 phosphorylation of one or more target proteins could play an important role in formation/extension of the cell wall, or in closely associated processes, such as cell division.

Directed yeast 2-hybrid analysis showed that MPK20 can physically interact with MKK9, and *in vitro* phosphorylation assays using recombinant proteins showed that a 'constitutively active' form of MKK9 is able to phosphorylate, and activate, MPK20 [48]. However, the *in planta* targets of MPK20 remain unknown, and exactly how MPK20 might be involved in primary cell wall biogenesis is also unclear, although a number of possibilities can be considered.

Two primary cell wall CesAs, including CesA3, possess canonical MAPK phosphorylation target sites (PXS/TP), which might indicate that MAPK-catalyzed phosphorylation influences the function of these enzymes. However, in exploratory experiments, crude recombinant MPK20 does not appear to be able to phosphorylate recombinant CesA3 *in vitro*, although this needs to be confirmed (Dr. Albert Cairo, unpublished data). Since the CesA3 protein has also been shown in phosphoproteomic profiling studies to be phosphorylated on multiple sites, including non-MAPK target sites [63], it is possible that MAPK-catalyzed phosphorylation can only occur after prior phosphorylation at one or more other sites.

Data deposited in MIND0.5 (Membrane-protein Interaction Network Database 0.5) also shows that MPK20 physically interacts with AtPIN1 in the mbSUS assay system (Mating-based split-ubiquitin system). AtPIN1 has multiple phosphorylation sites according to phosphoproteomics analysis; it is phosphorylated by AtPINOID [64], and the PIN1 protein also has multiple potential MAPK substrate motifs (T/SP). These observations suggest that MPK20 might influence one or more auxin-related pathways via phosphorylation of AtPIN1 [65].

Rice possesses multiple paralogous forms of MPK20 [66]. Recently, OsWRKY30 was shown to interact with OsMPK20-4/OsMPK20-5 in Y2H assays [67]. Expression of *OsWRKY30*, which contains two WRKY domains and is a member of Group Ia of the rice WRKY family, is rapidly induced by SA, JA and pathogen (*M. grisea)* infection. The authors suggest that the OsMPK20-4/5 isoforms may be involved in a JA or SA pathway by regulating OsWRKY30 phosphorylation.

An Arabidopsis *mpk20 KO* mutant appears to grow and develop normally (see Results), but since MPK20, MPK19 and MPK18 are close paralogues (Figure 1.5), they may share some functional redundancy, which can make analysis of single knock-out mutant phenotypes problematic. However, unlike *MPK20*, *MPK19* expression is correlated more closely with floral development than with primary cell wall formation (personal communication: Marcus Samuel, U. Calgary), suggesting that at least these two paralogous MPKs have diverged functionally since their ancestral duplication. MPK18 and 19 are even more closely related, but can still be functionally distinguished at some level, since whereas MPK18 interacts with the MAPK phosphatase, PHS1, in Y2H assays, MPK19 does not [48]. PHS1 was also shown to be able to de-phosphorylate recombinant MPK18 *in vitro* [68], but its activity against MPK19 or MPK20 has not been tested. Interestingly, PHS1 has recently been shown to possess protein kinase activity against specific cytoskeletal proteins [69], as well as its cognate phosphatase activity.

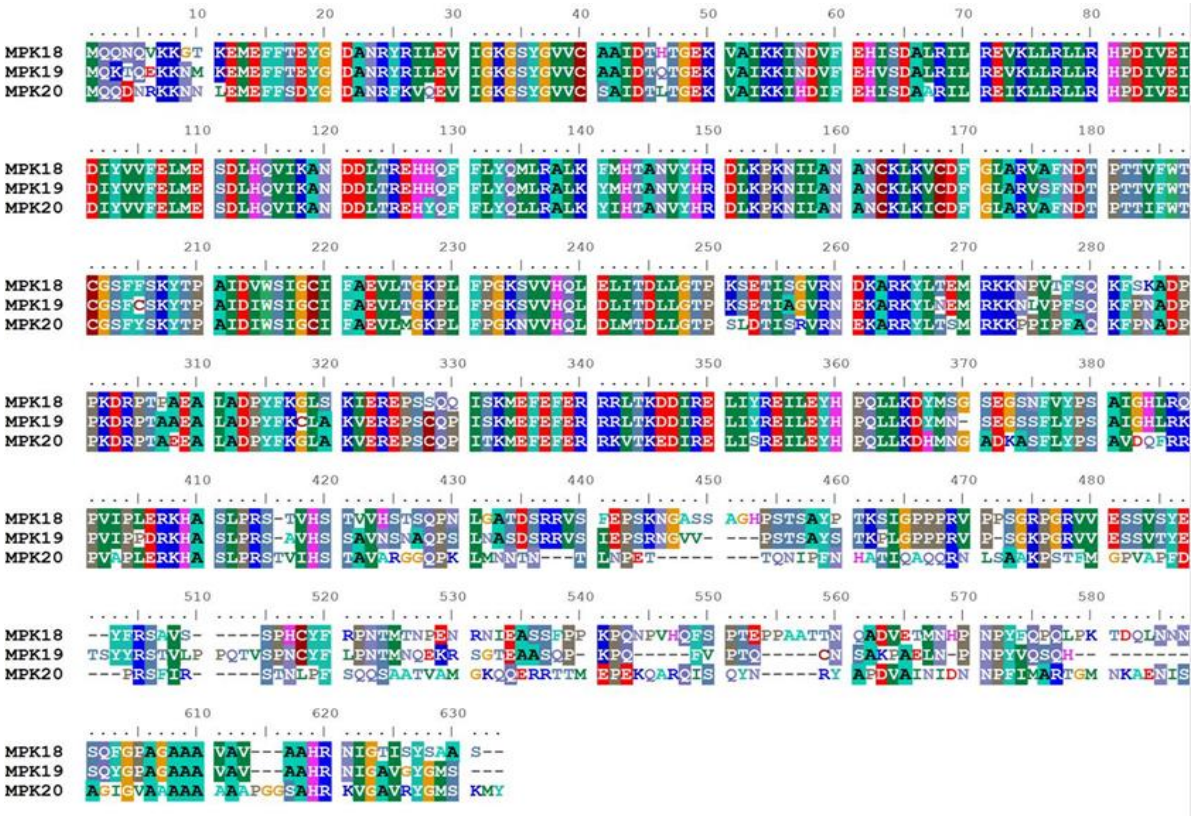


**Figure 1.5: Alignment of MPK18, 19 and 20 amino acid sequences.**

The sequences were aligned via Clustal X. The three MPK amino acid sequences are the same up to the 440$^{th}$ amino acid.

MPK18, 19 and 20 are paralogues, since their amino acid sequences are highly similar to each other (analysis in Clustal X). The alignment shows that most part of the three MPKs have the same amino acids, whereas the C-terminals are divergent.

### 1.2.5 MPK20 and plant primary cell walls

The plant cell wall is essential for resisting turgor pressure. There are two types of plant cell walls: primary cell walls and secondary cell walls. In the primary cell wall, the basic structural component is a polymer of glucose residues called cellulose, a composite of paracrystalline β-1,4-glucan chains. Cellulose polymers form linear chains that are hydrogen-bonded side by side to create linear, semi-crystalline structures named cellulose microfibrils [70]. Cellulose is synthesized by the cellulose synthase complex (CSC), which has a rosette-like structure at the plasma membrane and extends into cytoplasm, and is associated with cellulose chains. These chains bind together to form the cellulose microfibril [71]. Freeze fracture studies revealed that the rosette has a six-lobed structure [72, 73]. By using co-immunoprecipitation, it was confirmed that the primary cell wall CSC contains three CesA subunits – CesA1, 3 and 6 [74]. Among them, CesA1 and 3 show unique functions, as *knock out* mutations of these genes are gametophytic lethal [75]. In contrast, CesA6 mutants only have mild phenotypes, such as a short root and hypocotyl [76].

Previous studies showed that MPK20 may be involved in primary cell wall-associated biochemical processes. According to data from several hundred microarray experiments, *MPK20* expression is correlated with the expression of *AtCesA1*, *3* and *6*, the putative primary cell wall CesAs (Figure 1.6). Moreover, in the ATTED gene co-expression database [77-79], expression of four genes is directly correlated with expression of MPK20: COB (At5g60920, COBRA, extracellular glycosyl-phosphatidylinositol-anchored protein family), RSW1 (At4G32410, Cellulose synthase 1), SRF3 (At4g03390, STRUBBELIG-receptor family 3), and BIM1 (At5g08130, basic helix-loop-helix DNA-binding superfamily protein) (Figure 1.7).

| *Arabidopsis* Genome Initiative no. | Protein homology | Scor |
|---|---|---|
| 5G05170 | Cellulose synthase, *CESA3* | 6 |
| 4G32410 | Cellulose synthase, *CESA1* | 7 |
| 5G64740 | Cellulose synthase, *CESA6* | 8 |
| 5G60920 | *COBRA* | 9 |
| 1G76670 | Transporter-related | 45 |
| 1G04430 | Dehydration-responsive like | 47 |
| 1G05850 | Chitinase-like protein 1 (*CTL1*) | 47 |
| 4G26690 | Glycerophosphoryl diester phosphodiesterase family protein | 49 |
| 1G29470 | Dehydration-responsive like | 64 |
| 4G39350 | Cellulose synthase, *CESA2* | 69 |
| 1G12500 | Phosphate translocator-related | 79 |
| 5G35160 | Endomembrane protein 70 | 106 |
| 3G62660 | Glycosyl transferase family 8 protein | 130 |
| 4G39840 | Expressed protein | 149 |
| 2G41770 | Expressed protein | 171 |
| 1G58440 | Squalene monooxygenase | 174 |
| 4G31590 | Glycosyl transferase family 2 protein | 179 |
| 4G18030 | Dehydration-responsive protein | 185 |
| 5G01460 | LMBR1 integral membrane protein | 188 |
| 4G03390 | Leucine-rich repeat protein kinase | 194 |
| 1G45688 | Expressed protein | 198 |
| 2G42880 | Mitogen-activated protein kinase | 220 |

**Figure 1.6: Top 22 genes that are co-regulated with CesA1, 3, and 6 [62].**

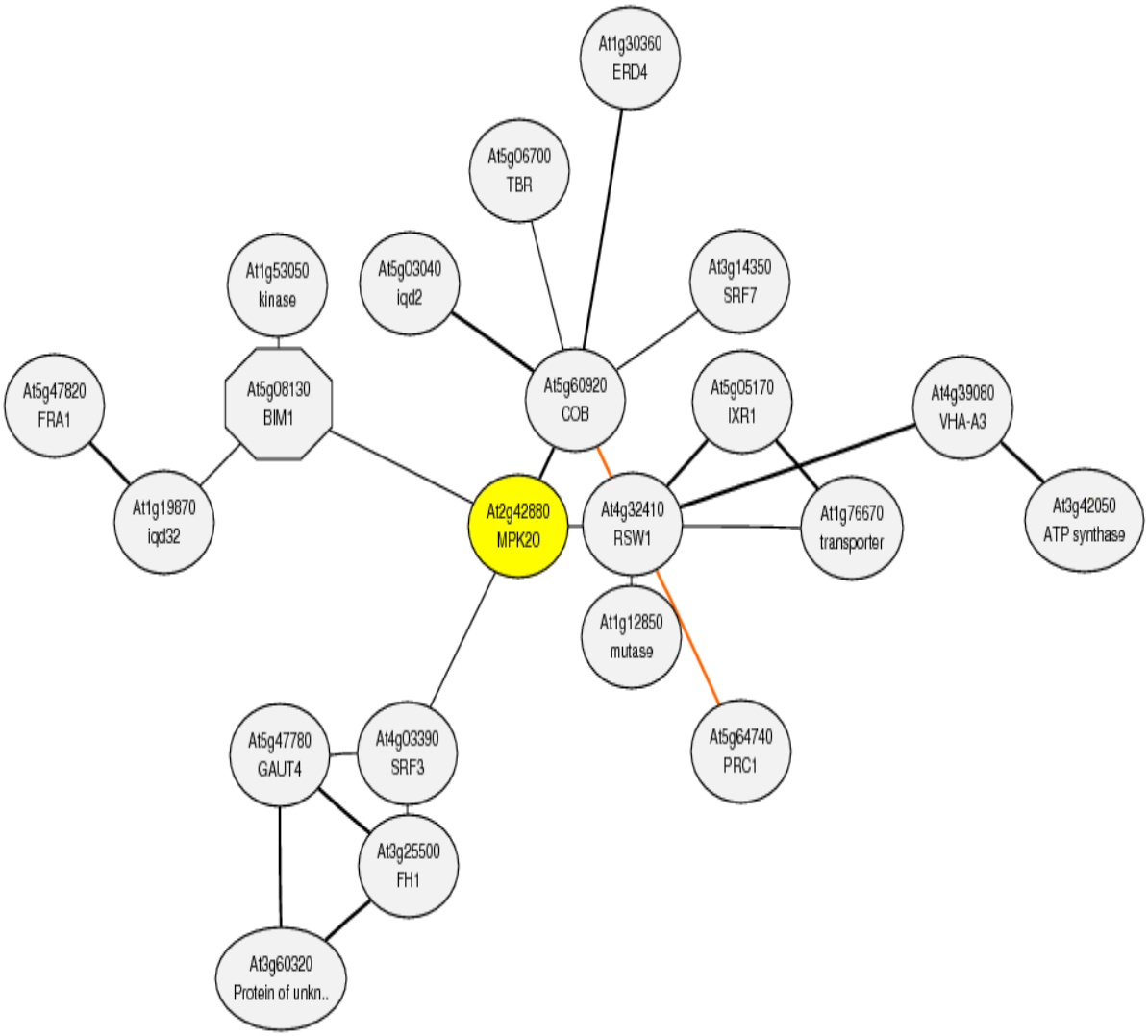


**Figure 1.7: Co-expression network around *MPK20* (ATTED database).**

The developmental pattern of *MPK20* gene expression also seems to support the hypothesis that MPK20 is somehow involved in primary cell wall formation. The e-FP browser [80] information shows that, although the *MPK20* gene is generally expressed in all plant growth stages and tissues, it is somewhat more highly expressed in the hypocotyl and root in *Arabidopsis* seedlings (Figure 1.8). The results of a previous *Arabidopsis* inflorescence stem gene expression profiling study conducted in our lab (Hall, unpublished data), on the other hand, showed that the expression of MPK20 does not vary very much between stem tissues of different growth stages:

young stage, maximum growth-rate stage, cessation stage and post-cessation stage. This could indicate that MPK20 may be involved in primary cell wall biosynthesis predominantly during the seedling stage.

Two studies in poplar have provided additional indications that MPK20 might be important in cell wall development. By analyzing the correlations between a range of phenotypic traits and occurrence of genome sequence polymorphisms (especially SNPs (Single nucleotide polymorphisms)), a correlation was found between three SNPs for the poplar *MPK20* homologue and the insoluble lignin content of the wood (Douglas and Mansfield, unpublished data). Moreover, the expression of the poplar *MPK20* gene is down-regulated when the xylem tissue develops into tension wood (Sundberg, unpublished data). These clues are consistent with a hypothesis in which MPK20 gene expression decreases as secondary cell wall formation occurs, and the cell is no longer actively synthesizing a primary cell wall.

## 1.3 Project objectives

Although group D has many MPK members, very little is known about the role of this group of MPKs in Arabidopsis. A number of previous studies have indicated that MPK20 might participate in cell wall formation and/or associated pathways, especially in Arabidopsis seedlings. In my studies, I focused on finding the biological function of MPK20 in Arabidopsis, using predominantly a reverse genetics strategy, and driven by the hypothesis that MPK20 is involved in a primary cell wall metabolic pathway. As well as examining the single mutants for MPK18, 19 and 20, the phenotypes of mpk18 mpk20, mpk19 mpk20 and mpk18 mpk19 double KO mutants were also explored, to try to circumvent potential redundancy of MPK function among MPK18, MPK19 and MPK20. In addition, the hormone responsiveness of mpk20 mutants was investigated, since several MPKs work in phytohormone-related pathways, and AtPIN1, for example, might be a substrate of MPK20. Finally, an attempt was made to prepare purified recombinant MPK20 protein so as to be able to test whether MPK20 interacts with and/or phosphorylates AtPIN1 in vitro.

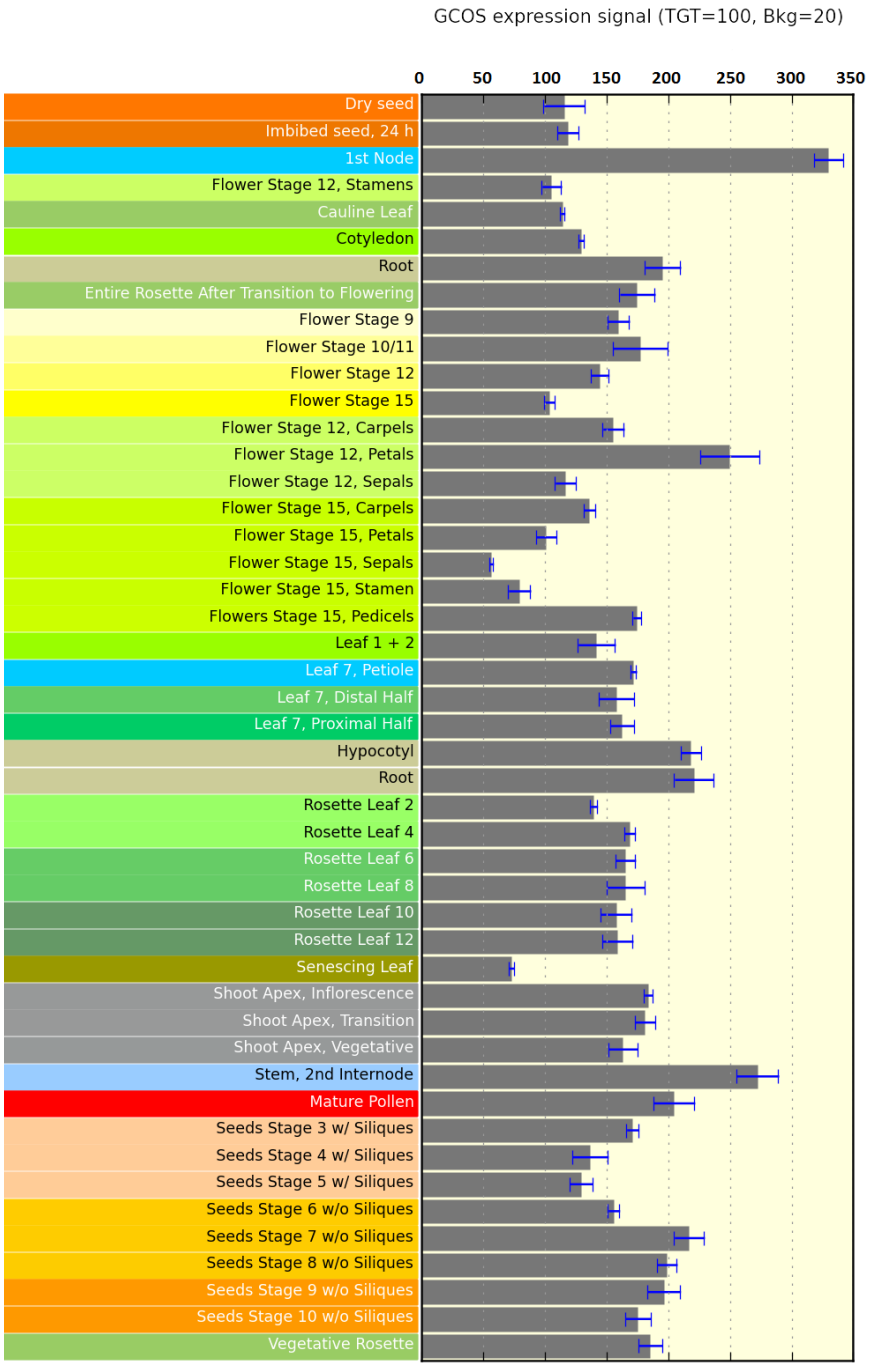


**Figure 1.8: e-FP browser information about *MPK20* expression pattern (e-FP browser).**

# 2 Materials and methods

## 2.1 Plant materials

Ecotype Col-0 (Columbia-0) was used as the control (WT) line. The knock out mutants of *MPK20*, (*mpk20*-2 and *mpk20*-3), and the knock out mutant of *MPK19*, *mpk19*-3, were provided by Dr. Marcus Samuel (University of Calgary). These three mutants are all T-DNA insertion mutants in the Col-0 ecotype background, but the *mpk20* mutants are SALK lines whereas the *mpk19* mutant is a SAIL line. Another T-DNA insertion mutant *mpk20-1* (SALK_036317) was ordered from ABRC (Arabidopsis Biological Resource Center). The knock out mutant of *MPK18*, *mpk18*-1, is a SALK line mutant and was previously used in our lab [68].

## 2.2 Plant growth conditions

For all experiments, Arabidopsis seeds were first treated by gas sterilization as described in [81]. Briefly, this involved putting two beakers in a sealable container, each beaker containing 100mL undiluted commercial bleach, and slowly adding 3mL HCL to each beaker. About 0.3mL Arabidopsis seeds from each line were put into a 1.5mL microtube. The microtube was left uncapped and placed horizontally in the container, which was sealed for 2h-4h depending on the number of seeds.

After being stratified at 4 ℃ for 2 days, the sterilized seeds were germinated on ½-strength Murashige and Skoog (MS) medium plates (2.2 g/L 1/2 MS salts, 0.25 g/L MES, and 8 g/L agar, pH 5.7) in the growth room at 22-24 ℃ under 16h/8h photo-period, with constant white light.

## 2.3 DNA extraction and Polymerase Chain Reaction (PCR) for genotyping

For genomic DNA extraction, 100 mg 7d-old seedlings were ground into powder in liquid nitrogen. DNA extraction buffer (400 μL) (200 mM Tris-HCl, pH 7.5, 250 mM NaCl, 25 mM EDTA, 0.5% SDS) was added to the homogenized powder and stirred briefly as it thawed.. After centrifugation at 13,000 rpm 7500 g for 1 min, 400 μL isopropanol was added to the supernatant for DNA precipitation. After further centrifugation at 13,000 rpm for 5 min, the precipitate was washed with 700 μL 70% ethanol and re-centrifuged at 13,000 rpm for 5 min. After removing the ethanol supernatant and allowing any residual ethanol to completely evaporate by standing at room temperature, 40 μL $dH_2O$ was added for DNA resuspension.

For genotyping, 4 μL of this DNA solution was used as template, together with the primer sets listed in Table 2.1. All primers were obtained from IDT. The PCR product was later run on a 1% agarose gel (adding 0.5g agarose into 50mL TAE (Tris-Acetate-EDTA)).

Primers *mpk20-1.F* and primer *Lbb1* were used to confirm whether *mpk20-1* contains a T-DNA insertion, while primer *mpk20-1.F* and primer *mpk20-1.R* were used to amplify the full *MPK20* gene sequence. When DNA from Col-0 genotype plants was used as the template in PCR, the former primer combination produced no band in the DNA gel, whereas the latter primer set showed a clear band at the expected molecular mass. If the *mpk20-1* line produces a normal *MPK20* gene amplicon, it must lack a T-DNA insertion, and this line will have a functional *MPK20* mRNA sequence; i.e. it will not be an *mpk20 ko* mutant (Figure 3.2b).

For checking the absence of *MPK20* transcripts in *mpk20-2* plants, the combination of primer *mpk20.M1* and *Lbb1* was used to confirm the T-DNA insertion, and the combination of primers *mpk20.M1* and *mpk20.R1* was used to check the absence of *MPK20* full-length gene sequence. To confirm that *mpk20-3* is an *mpk20 ko* mutant, primer *mpk20.F1* and primer *Lbb1* were used to check the T-DNA insertion, while primer *mpk20.F1* and primer *mpk20-3.R* were used to amplify the *MPK20* gene sequence.

Primers *RP* and *Lbb1* were used to genotype plants grown from homozygous *mpk18-1* (SALK_069399) seeds, while the combination of primers *Lb1* and *mpk19R2* were used to genotype the *mpk19-3* (SAIL_544_G10) seedlings.

For collecting PCR product from agarose gels, the UV-illuminated band was cut from the agarose gel and extracted by using the QIAquick Gel Extraction Kit (Cat # 28706, QIAGEN).

For gene sequencing, 100ng of gel extraction product was sent to IDT for gene sequencing.

## 2.4 RNA extraction and semi-quantitative reverse-transcription PCR (SQ RT-PCR)

For total RNA extraction, 14d-old seedlings (1g) were ground into powder in liquid nitrogen. Trizol reagent (1mL) was added to the frozen powder and allowed to stand for 5 min at room temperature. After 200 μL chloroform was added for partitioning RNA into the aqueous phase, the 1.5 mL centrifuge tube was shaken briskly for 5 sec. After standing at room temperature for another 2 min, the tube was centrifuged at 13,000 rpm for 15 min at 4 ℃. After the aqueous phase was transferred to a new tube, 500 μL isopropanol was added for RNA precipitation and the tube was allowed to stand for 10 min at room temperature. After centrifugation at 13,000 rpm for 15 min at 4 ℃, the RNA pellet was washed with 75% ethanol and the tube was centrifuged again at 9000 rpm for 5 min at 4 ℃. After the ethanol supernatant was removed and residual solvent had completely evaporated, the pellet was re-suspended in 20-30 μL diethylpyrocarbonate (DEPC)-treated $dH_2O$ (autoclaved with 0.05% DEPC and allowed to stand for 24h before being used).

For RT-PCR, 1 μg total RNA was used for synthesizing cDNA by using the SuperScript® II Reverse Transcriptase Kit (Cat # 18064-014, Invitrogen). For SQ (semi-quantitative) RT-PCR, 0.5μl cDNA was used as template, together with the primer sets listed in Table 2.2.

Even if *mpk20 ko* plants have the T-DNA insertion interrupting the normal *MPK20* gene sequence, SQ RT-PCR is necessary to confirm that no *MPK20* RNA is being transcribed in *mpk20 ko* plants. Thus, the primer combination of *mpk20.MF1* and *mpk20.MR1* was used to

check if the total RNA from *mpk20 ko* plants (*mpk20-1, mpk20-2,* and *mpk20-3*) contains *mpk20* mRNA sequence or not. Two other primers sets were used for this purpose, as well: *mpk20.MF1* plus *mpk20.R1*, and *mpk20.F1* plus *mpk20.MR1* (Figure 3.2c).

For confirming the status of *mpk18* and *19 ko* mutants, two sets of primer were used: *mpk18F* and *mpk18R* for checking *MPK18* cDNA; whereas *mpk19F* and *mpk19R* were used for amplifying *MPK19* cDNA.

## 2.5 *ProMPK20::GUS* lines

There have been no formal studies of the *MPK20* promoter, so to obtain an *MPK20* promoter, a 2 Kbp region upstream of the transcriptional start codon of the *MPK20* open reading frame was usedfor constructing a *ProMPK20::GUS* plasmid. The cloned promoter fragment was inserted into the pMDC162 vector by Gateway cloning: the promoter fragment was first amplified from *Arabidopsis* genomic DNA by using primer set *MPK20promoter.F.1* (AAAAAGCAGGCTATTT-TTGAGAGCTTATATGATCC) and *MPK20promoter.R.1* (AGAAAGCTGGGTCGTGAC-TCAATTGAAACACAG). This PCR product (1 μL) was used as template and amplified by primer set *attB1* (CAAGTTTGTACAAAAAAGCAG) and *attB2* (CCACTTTGTACAAGAAAGCTG) by PCR. The resulting PCR product was cloned into pDONR$^{TM}$221 by BP reaction, and then an LR reaction was performed for transferring *MPK20* promoter fragment into pMDC162.

The *pMDC162/ProMPK20* construct was transformed into Col-0 plants (T1), and the T2 plants were genotyped by PCR for selection of homozygous lines. Selected homozygous T3 seedlings were used for GUS staining by immersion in X-Gal staining buffer (5-bromo-4-chloro-3-indolyl-β- D-glucuronide cyclohexylammonium salt, 50 mM phosphate buffer, 5 mM $K_3/K_4FeCN$, 0.1% Triton X-100, pH 7) at 37 ℃ for 1-2h. The stained samples were held at 4℃ overnight, washed in 96% ethanol and examined on a Zeiss Axioplan Fluorescence Microscope.

## 2.6 Recombinant protein expression in *E. coli*

A full-length *MPK20* cDNA was cloned into either the pGEX4T-1, pET-28 or pEXP1-DEST vectors, and the resulting plasmid DNA was transformed into One Shot® BL21 (DE3) cells. After selecting the cells on LB plates containing the appropriate antibiotics (kanamycin for pET-28; ampicillin for pGEX4T-1 and pEXP1-DEST), a colony was picked and incubated in 5mL LB + appropriate antibiotics at 37 ℃ overnight. A 1mL aliquot from this culture was used to inoculate a 250mL flask containing 50mL LB medium plus antibiotics. This flask was placed on a 37 ℃ gyratory shaker for 3 to 5 hours, until the $OD_{600}$ of the culture was around 0.4 ~ 0.6 OD. The culture was then treated with IPTG (0.5mM final concentration) to induce expression of the cloned gene in the bacterial cells, and the flask was incubated further on a 22 ℃ shaker overnight.

For analyzing the size of the extracting protein, SDS-PAGE (sodium dodecyl sulfate - polyacrylamide gel electrophoresis) was performed. A combination of 10 mL 10% resolving gel (4 mL $H_2O$, 3.3 mL 30% acrylamide mix, 2.5 mL 1.5M pH8.8 Tris-Cl, 0.1 mL 10% SDS, 0.1 mL 10% ammonium persulfate and 4 μL TEMED (tetramethylethylenediamine)) and 6 mL 5% stocking gel (4.1 mL $H_2O$, 1 mL 30% acrylamide mix, 0.75 mL 1M pH6.8 Tris-Cl, 0.06 mL 10% SDS, 0.06 10% ammonium persulfate and 6 μL TEMED) was used in the system.

The crude protein extract (2 μL) was mixed with 8 μL protein loading dye in one tube and held in boiling water for 10 min. After loading the gel, it was run at 14 mA until the loading dye ran out from the bottom.

For Coomassie Blue staining, the SDS-PAGE gel was immersed in Coomassie staining (500 mL $H_2O$, 100 mL glacial acid, 400 mL methanol, and 1 g Coomassie R250 dye) buffer for 1 hour at RT. The gel was subsequently washed at least three times (until clear) by using destaining buffer (300 mL ethanol, 600 mL $H_2O$ and 100 mL acetic acid).

For western blotting, the SDS-PAGE gel and the PVDF (polyvinylidene difluoride) membrane were clamped together and run in transfer buffer (700 mL H2O, 200 mL methanol, 100 mL 10X transforming buffer (144 g glycine, 30.2 g Tris base and 900 mL $H_2O$)) at 100 V, 4 ℃ for one hour. The membrane was then immersed in a skim milk buffer (50 mL PBST (Phosphate

Buffered Saline Tween - 20) and 2.5 g skim milk powder) to block cross-reaction and shaken for 1 hour at RT. It was then transferred into blocking buffer containing 0.1% of the appropriate antibody for the vector epitope tag, and shaken overnight at 4 °C. After washing the membrane in PBST, it was immersed in milk buffer containing 0.02% the secondary (anti-mouse) antibody and shaken for 1 hour at RT. The membrane was then washed with PBST four times and placed in PBS. Antibodies bound to the membrane were detected by using Novex® ECL Chemiluminescent Substrate (Cat # WP20005, Invitrogen)

**Table 2.1Primers used in genotyping**

| primer name | primer sequence |
|---|---|
| mpk20-1.F | GGGTTGTTTTTTTGGATCACAG |
| mpk20-1.R | CGCCTAATGAAGGATCAATG |
| LBb1 | GCGTGGACCGCTTGCTGCAAC |
| mpk20.M1 | GGAGTATAGGCTGCATTTTTGC |
| mpk20.R1 | TGAAAGCCCAGCTTAGGTGG |
| mpk20.F1 | GCACATTATGCTTCCTCCTTCACGA |
| mpk20-3.R | TGAATGCAACCCTTGCCAATCCA |
| RP | GATCAAAAGCATTATGCTGCC |

| primer name | primer sequence |
|---|---|
| LP | TTTTGGTGTGCCAAGAAGATC |
| LB1 | GCCTTTTCAGAAATGGATAAATAGCCT TGCTTCC |
| MPK19.F | TACGACAGTCTTTTGGACGG |
| MPK19.R.1 | TAGGATATAGAAAACTTGAGCC |

**Table 2.2Primers used in SQ-RT-PCR**

| primer name | primer sequence |
|---|---|
| mpk20.MF1 | CCACCGAGACCTGAAACCA |
| mpk20.MR1 | CGGTCACTGATGTTTTCGGC |
| MPK18F | ATGCAACAAAATCAAGTGAAG |
| MPK18R | CTATGATGCTGCGCTGTAAC |
| MPK19.F | TACGACAGTCTTTTGGACGG |
| MPK19.R.2 | GGTTTGGCAGAGTTGCATTG |

| primer name | primer sequence |
|---|---|
| ACT.R | AGCAAGGTCAAGACGGAGGATG |
| ACT2.F | TCTTCCGCTCTTTCTTTCCAAGC |

# 3 Results

## 3.1 Gene expression pattern of *MPK20* in *Arabidopsis* seedlings

The hypothesis that MPK20 is associated in some fashion with cell wall-related processes could mean that this relationship is true for a very restricted set of circumstances, spatially or temporally (e.g. cellulose synthesis within a specific tissue or at a specific stage of development). Alternatively, the relationship might hold true much more broadly across the plant and its growth/development. In the first case, I would predict that the expression of the *MPK20* gene would be similarly restricted, but in the second scenario, I would predict that the gene would be far more generally expressed. To test these hypotheses, I examined the expression pattern of the *MPK20* promoter in *Arabidopsis* seedlings by using transgenic *Arabidopsis* lines expressing a GUS reporter construct driven by a 2kb *MPK20* promoter.

The GUS staining pattern of these transformed *Arabidopsis* seedlings showed that the *MPK20* promoter was active in true leaves, cotyledons, hypocotyl, primary root tips, sites of emerging lateral roots, and in lateral root tips (Figure 3.1). While staining was more intense in the vascular strands than in ground tissue, the overall pattern confirmed that the *MPK20* gene is widely expressed through all organs of *Arabidopsis* seedlings, including roots and hypocotyl.

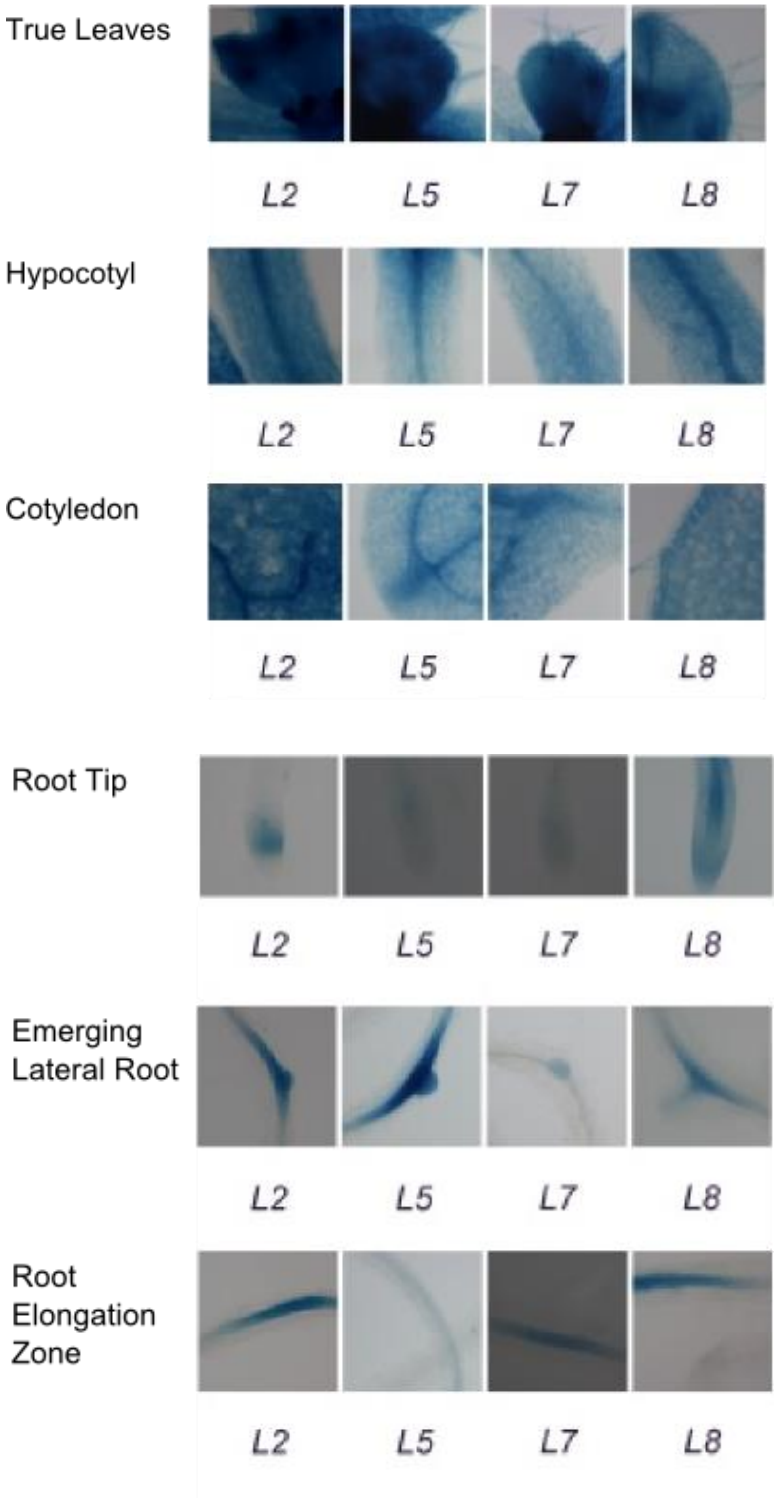


**Figure 3.1: Expression pattern of the *MPK20* promoter in transgenic *Arabidopsis* seedlings.**

Four homozygous transgenic *Arabidopsis* lines expressing a *ProMPK20::GUS* construct were selected for GUS staining (L2, L5, L7 and L8). These lines were grown on 1/2MS plates for 10 days and the whole seedlings were then stained.

## 3.2 Selecting *mpk20 ko* mutants

For the *MPK20* gene, there were three putative T-DNA insertion mutant lines available in the public Arabidopsis mutant collections (*mpk20-1* SALK_036317, *mpk20-2* SALK_148463, and *mpk20-3* SALK_146654), but these each needed to be examined for their true mutant status, and for their homozygosity. Several primers were therefore designed for selecting *mpk20 ko* mutants by PCR-based genotyping (Figure 3.2a).

The gel image of PCR-based genotyping shows that *mpk20-1* contains the T-DNA insertion and does not have the normal *MPK20* gene sequence (Figure 3.2b). However, *mpk20*-1 plants still appear to produce *mpk20* mRNA, according to the SQ RT-PCR results (Figure 3.2c). I therefore concluded that, *mpk20-1* is not an *mpk20 ko* mutant. The genotyping results and the gene sequencing results confirmed that *mpk20-2* contains the T-DNA insertion after the $3300^{th}$ bp and that *mpk20-3* contains the T-DNA insertion after the $813^{th}$ bp. Moreover, neither of the two mutants has the normal *MPK20* gene sequence or *mpk20* mRNA sequence (Figure 3.2). Consequently, from the three T-DNA insertion mutants tested, two *MPK20 knock out* mutants were finally selected for further research: *mpk20-2* (SALK_148463) and *mpk20-3* (SALK_146654) (Figure 3.2).

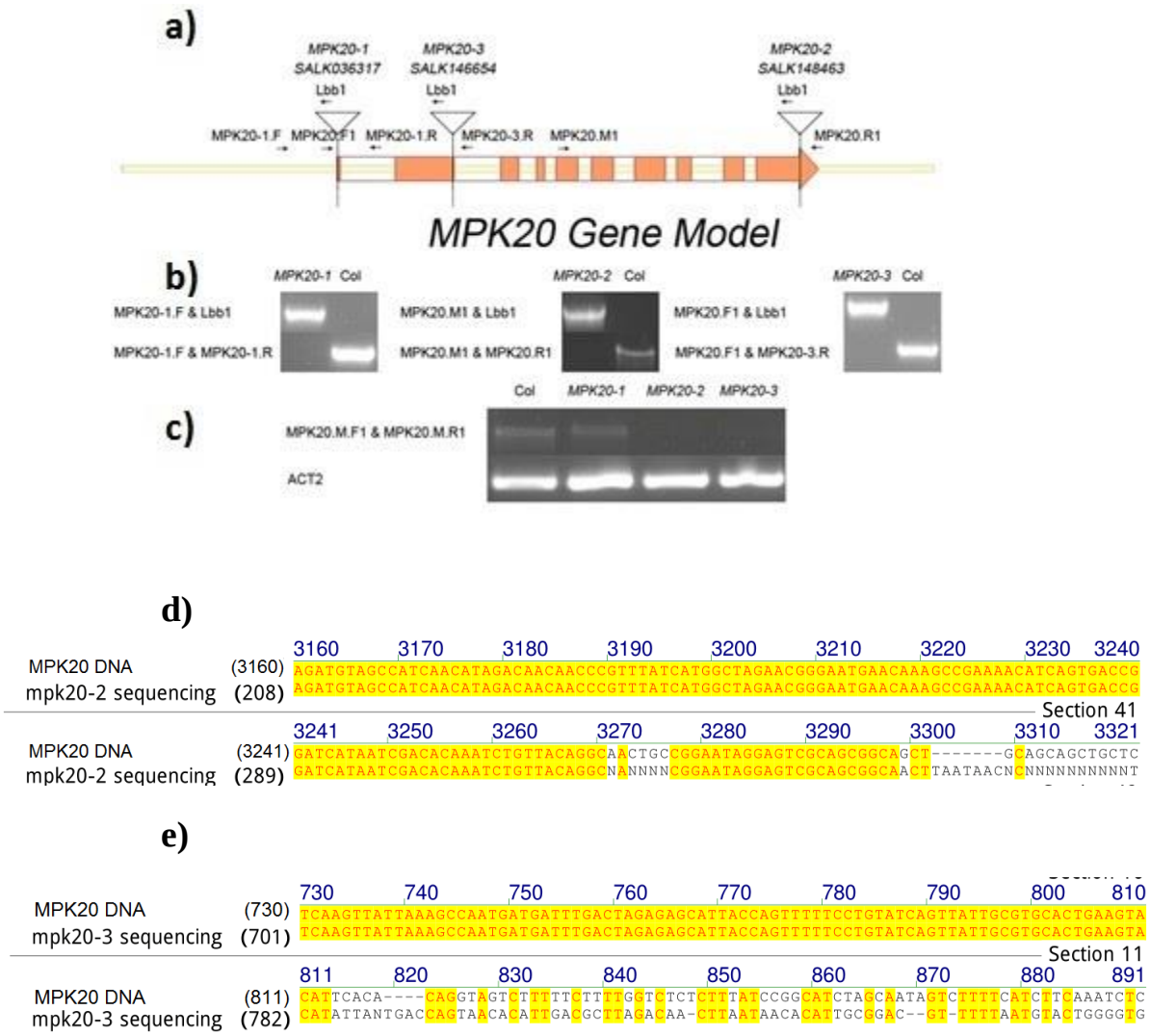


**Figure 3.2: Identification of *mpk20 ko* mutants.**

**a)** Gene model of *MPK20* and the T-DNA insertion position within three *mpk20* mutants. Arrows show the relative position of the various PCR primers.

**b)** Genotyping results for three mutants indicate that all three lines are homozygous T-DNA insertion lines.

**c)** SQ RT-PCR results for three mutants indicate that *mpk20-2* and *mpk20-3* are totally *mpk20 knock out* mutants.

**d)** Alignment of the *MPK20* DNA and the *MPK20* gene sequencing result for *mpk20-2*; the two sequences were the same up until bp 3300.

**e)** Alignment of the *MPK20* DNA and the *MPK20* gene sequencing result for *mpk20-3*; the two sequences were the same up to bp 813.

## 3.3 The germination rate of *mpk20 ko* mutants

Since the two *mpk20 ko* mutants selected for further study did not have any obvious growth or morphology phenotypes when germinated on 1/2MS medium or grown in soil, compared to Col-0 plants, a more detailed examination of their developmental traits was carried out. One of the traits that was of potential interest was the rate of hypocotyl elongation in dark-grown *mpk20* seedlings, since this process requires rapid deposition and extension of primary cell walls. If MPK20 were involved in primary cell wall metabolism in Arabidopsis seedlings, I could envision that loss-of-function at the *MPK20* locus might affect this hypocotyl extension.

However, simply measuring the hypocotyl length at a particular time-point post-germination can produce inaccurate results if the mutant seeds do not germinate at the same rate as WT (Col-0) seeds. Seed germination is influenced by a number of factors, most notably the phytohormone, ABA. High concentrations of ABA inhibit radicle growth during seed germination (Figure 3.3) [82], and several MPKs (such as MPK3, 4, and 6) are essential for ABA signaling in Arabidopsis [15, 35, 83, 84]. Exploration of the germination behavior of *mpk20 ko* mutants could therefore also reveal whether MPK20 is involved in ABA signaling.

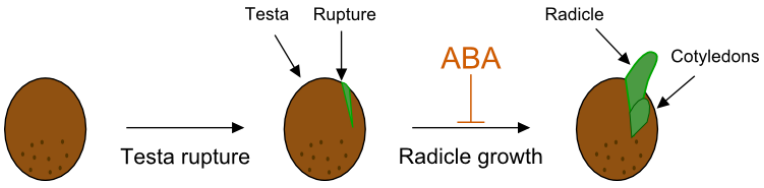


**Figure 3.3: ABA inhibits radicle growth during seed germination of *Brassica napus* [82].**

After comparing the germination timing of the two *mpk20* mutants with WT seeds, I confirmed that there was no significant difference between the germination rates of the seeds of all three

lines on 1/2MS plates, after 48-hour-stratification (Figure 3.4). Since the *mpk20 ko* mutants do not display an abnormal germination phenotype, I concluded that it would be reasonable to directly compare their dark-grown hypocotyl extension rates after dark germination. The absence of a significant impact of the *mpk20* mutations on the germination rates also suggested that MPK20 is not required for any ABA-related signaling pathway during seed germination.

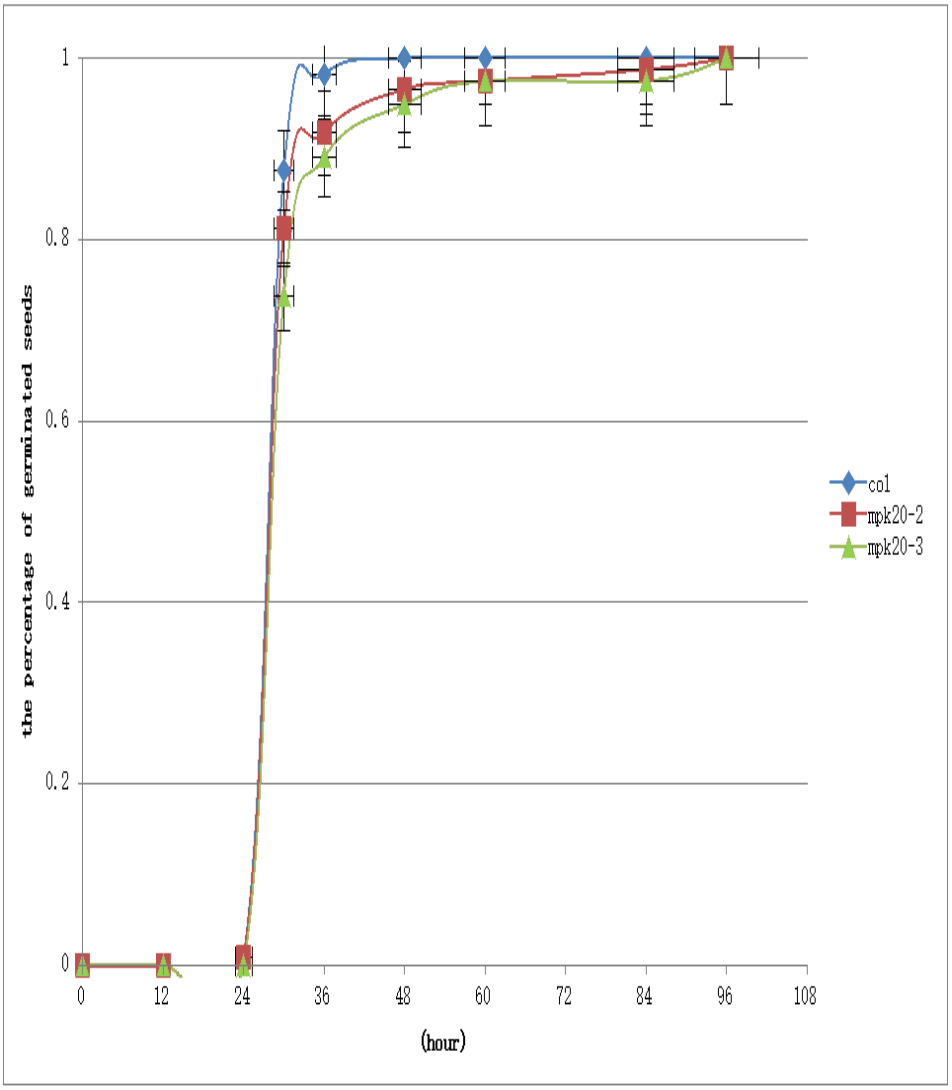


**Figure 3.4: The germination rate of Col 0 and *mpk20 ko* mutants at different times after 48 hours stratification.**

The seeds for the three lines (Col 0, *mpk20-2* and *mpk20-3)* were planted together on one 1/2MS Petri dish and stratified for 48 hours. The plate was then transferred to the growth room at 22-24 ℃ under 16h photoperiod constant white light, and germination was scored at various time-points after transfer. A seed was counted as germinated when the emerging radicle protruded a distance at least equivalent to the seed length. Each plate contained 50 seeds from each line, two plates were scored in each experiment, and three independent experiments were performed (300 seeds from each line in total). By t-test analysis (0.05 p value cut-off), the seed germination rate of the two *mpk20* mutants did not differ significantly from that of Col-0 seeds.

## 3.4 Hypocotyl elongation of dark-grown etiolated *mpk20 ko* mutants

As shown in the promoter-reporter experiments, the *MPK20* promoter is active in the hypocotyl, and expression of *MPK20* transcripts seems to be associated with primary cell wall biosynthesis. I therefore wanted to examine the hypocotyl extension phenotypes of plants lacking MPK20.

Arabidopsis seedling hypocotyls remain relatively short when the seedlings are grown in light, compared with those grown in the dark. However, this difference in hypocotyl dimensions is not the result of production of extra cells during dark growth; indeed the full complement of cells making up the hypocotyl is initially established through cell proliferation during embryogenesis. After seed germination, any elongation of the hypocotyl, in light or dark, is accomplished primarily through the expansion of these initial cells [85-88]. Since dark-grown hypocotyls are much longer, and therefore more easily measured, I grew the mutant and WT seedlings in the dark in order to collect data on their hypocotyl extension growth.

To more carefully monitor the changes in the seedlings, the hypocotyl length was measured at different time points (Figure 3.6). The plates of germinating seeds were positioned so that the surface of the growth medium was 75 degrees off the horizontal, which allowed the hypocotyls to grow free of the medium. The plates were kept in the dark until 3d, 4d, 5d or 7d after sowing, and at each time-point the length of each seedling hypocotyl was measured by capturing a digital image of a lateral view of the seedling, and measuring the hypocotyl length using Image J software (Figure 3.5) [89].

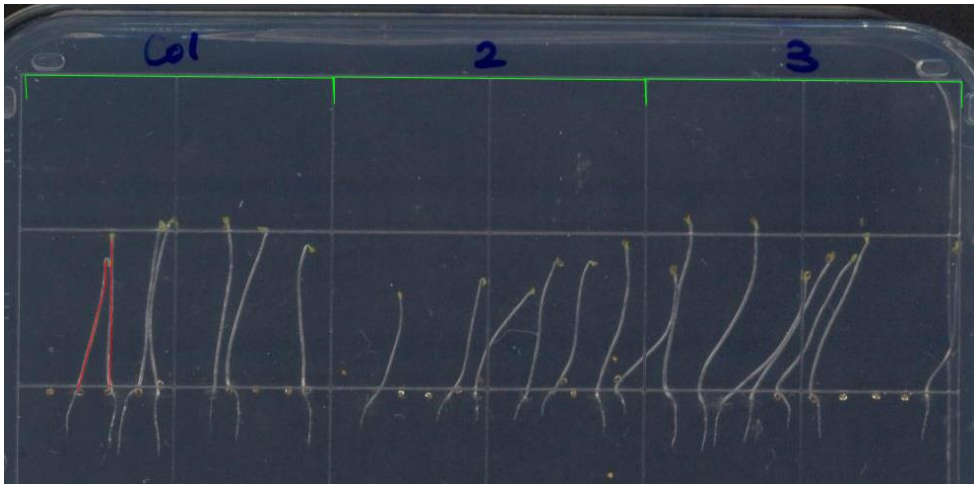


**Figure 3.5: Hypocotyl elongation of dark-grown 5-day-old etiolated Col 0 and *mpk20 ko* mutants.**

The hypocotyls of Col0, *mpk20-2*, and *mpk20-3* seedlings are labeled as "Col", "2", and "3", respectively. The red lines show the lengths of the hypocotyl that were used for measuring and further statistical analysis.

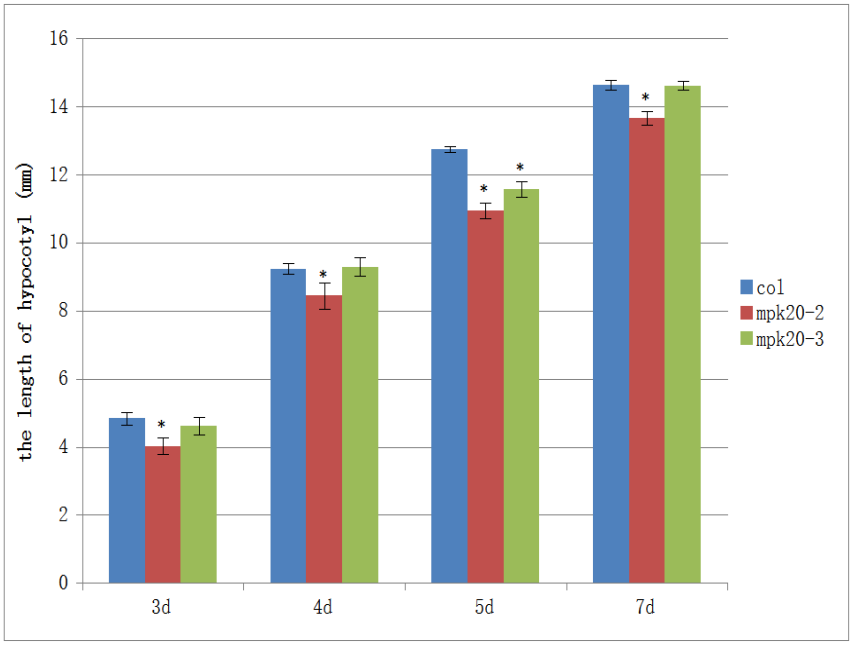


**Figure 3.6: Hypocotyl elongation of dark-grown etiolated Col 0 and *mpk20 ko* mutants.**

The seedlings were grown in the dark on 1/2MS plates for 3d, 4d, 5d or 7d at 22-24℃ before the measurement. Each bar in the figure represents the average hypocotyl length of approximately 100 seeds from each line, which were collected at four different time-points. At each time-point, three plates of seedlings were measured. Each plate contained 10 seeds of Col-0, 10 seeds of *mpk20-2* and 10 seeds of *mpk20-3*.

The length of *mpk20-3* hypocotyls is the same as that of Col 0 hypocotyls except at 7 days (significance assessed through t-test analysis, 0.05 p-value cut-off). However, *mpk20-2* seedlings consistently have shorter hypocotyls than *mpk20-3* or WT seedlings. The "*" mark indicates values statistically different from Col-0 (by t test analysis, 0.05 p value cut-off) and error bars indicate SD (standard deviation).

Although both *mpk20-2* and *mpk20-3* mutants lack *MPK20* mRNA transcripts, the average hypocotyl length in the two mutant lines was different over the period of the hypocotyl dark-growth experiments. The hypocotyl elongation of *mpk20-2* was shorter than *WT*, while that of *mpk20-3* was essentially the same as *WT*. When comparing only *mpk20-2* and *mpk20-3*, their hypocotyl lengths were not significantly different for 3, 4 or 5d-old seedlings, but for the 7d-old seedlings, *mpk20-3* hypocotyls were significantly longer than those of *mpk20-2*. Since both mutants are supposed to represent complete loss-of-function genotypes, the reasons for the differences between the *mpk20-2* and *20-3* seedlings are unclear. It is possible that one or both of

the mutants have multiple T-DNA insertions in their genomic DNA, with the additional insertion events having an impact on hypocotyl extension. Testing this hypothesis would require further line purification and analysis. In view of the small size of the observed differences in the hypocotyl extension phenotype, such an effort was not considered to be justified.

## 3.5 Root elongation is suppressed in one *mpk20 ko* mutant

As *MPK20* might be involved in cell wall-associated mechanisms in *Arabidopsis* seedlings, the primary root elongation rates of Col-0, *mpk20-2* and *mpk20-3* seedlings were compared. To avoid the effects resulting from individual variation in germination time-point, the differences between root lengths of 3-day-old and 7-day-old seedlings were measured. These are plotted in Figure 3.6 as blue bars. Similarly, the differences between 3-day-old seedling root length, and 14-day-old seedling root length are plotted as red bars.

The results showed that the average primary root length of *mpk20-2* seedlings is shorter than that of Col-0 seedlings, whereas *mpk20-3* plants have the same root length on average as Col-0 plants. The different behavior of the two *mpk20 ko* mutants is reminiscent of the results of the hypocotyl elongation experiment (Section 3.4), except that, in this case, the root lengths of *mpk20-2* and *mpk20-3* plants are statistically different from each other (Figure 3.7). Again, the basis of this difference in mutant phenotype is unclear, but the possibility remains that one or both T-DNA mutant lines could be carrying multiple insertions.

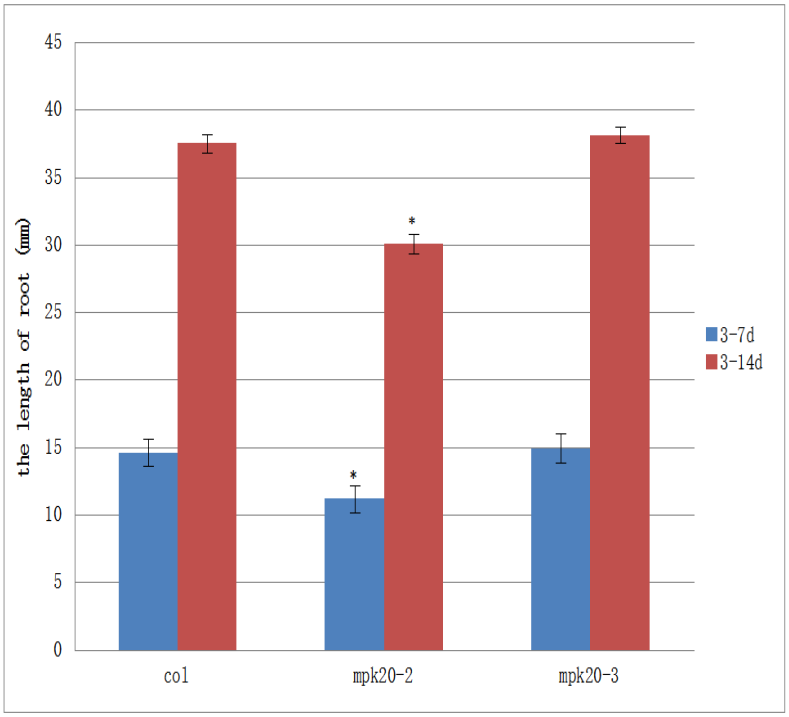


**Figure 3.7: The primary root growth of *mpk20 ko* mutants and Col 0.**

The primary root extension after the third day of growth was measured at the 7th day and 14th day. Root length was calculated from the results of three independent experiments using approximately 90 seedlings from each line. In each experiment, two plates of seedlings were scored. Ten seeds from each line were planted on the same 1/2MS plates and stratified for 48 hours. The plates were then positioned vertically in the growth room at 22-24 ℃ under a 16h/8h photo-period. Each experiment consists of three plates. The root length of *mpk20-2* is significantly shorter than that of Col 0 and *mpk20-3*. Moreover, there is also a statistically significant difference between *mpk20-2* and *mpk20-3*. The "*" mark indicates values statistically different from Col-0 (by t test analysis, 0.05 p value cut-off) and error bars indicate SD (standard deviation).

## 3.6 Building *mpk18*, *mpk19* and *mpk20* double mutants

Since neither of the *mpk20 ko* mutants has a strong phenotype in plant growth, primary root elongation or hypocotyl elongation, we must consider the possibility of protein functional redundancy. According to the Arabidopsis MPK phylogenetic tree (Figure 1.1 & 1.2), *MPK18*,

*MPK19* and *MPK20* are closely related paralogues; i.e. their amino acid sequences are almost identical, based on Clustal X analysis (Figure 1.3). Therefore, MPK18 and MPK19 are both candidate proteins which could potentially have some degree of redundant function with MPK20.

To test this idea, I first needed to confirm that *mpk18-1* (SALK_069399) and *mpk19-3* (SAIL_544_G10) are knock-out mutants, and then these two lines were each crossed with each other, and with one or both of the *mpk20* knock-out mutants (Figure 3.8). Various double mutant homozygous progeny were selected by PCR using the primer combinations described above, and are referred to as *mpk18-1 mpk19-3*, *mpk20-2 mpk19-3*, *mpk20-3 mpk19-3*, and *mpk20-2 mpk18-1*.

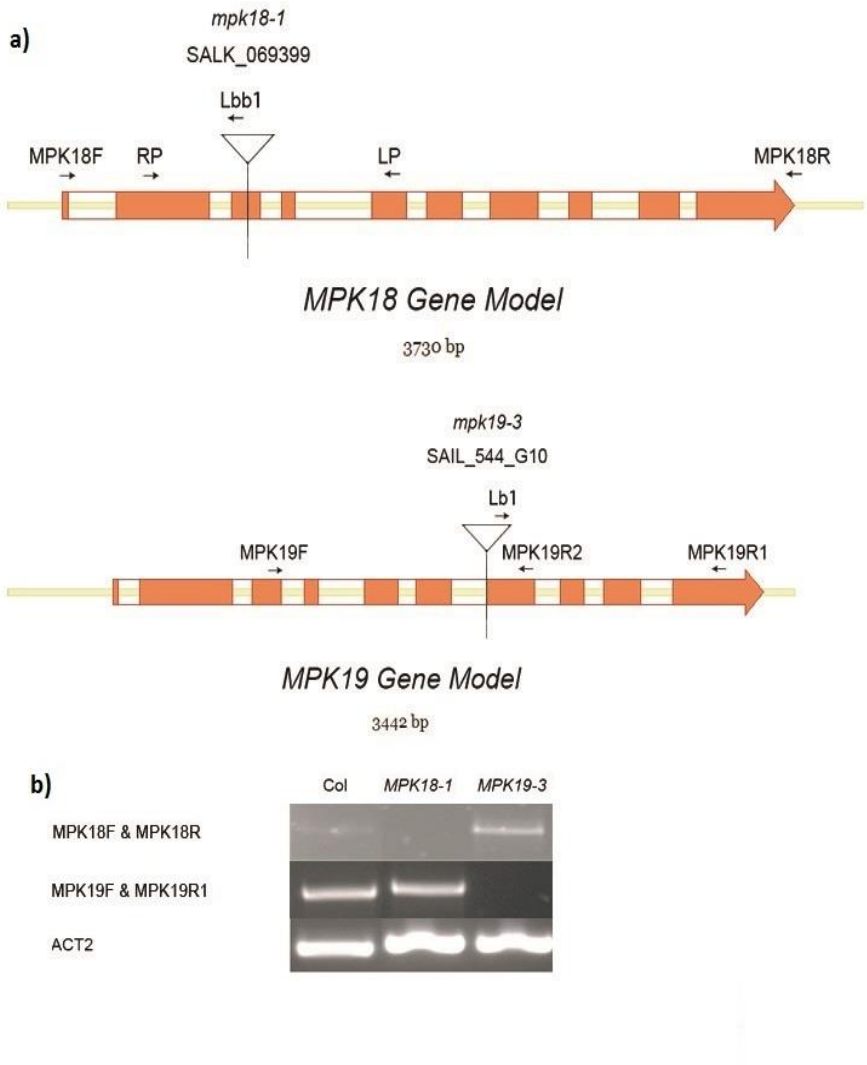


**Figure 3.8: Structures of the *MPK18* and *MPK19* genes in Arabidopsis.**

**a)** Gene models of *MPK18* and*MPK19,* and the T-DNA insertion position within the single mutants. Arrows show the relative place of the primers used for genotyping and SQ RT-PCR.

**b)** SQ RT-PCR results for the *mpk18* and *mpk19* mutants indicate that they are total knock-out mutants.

## 3.7 The phenotype of *mpk18*, *mpk19*, and *mpk20* double mutants

As individual differences in germination rate could affect the results of other growth experiments, the germination rates of all single and double mutants were tested from 0h to 108h (Figure 3.9).

The germination rates of the single and double mutants were generally not significantly different from that of Col 0, except in the case of the *mpk20-2 mpk18-1* double mutant which had lower germination at the 30h and 36h time points. Since only one line of each double mutant was examined, this apparent difference in the *mpk20-2 mpk18-1* germination phenotype needs to be confirmed though selection and testing of additional double mutant lines.

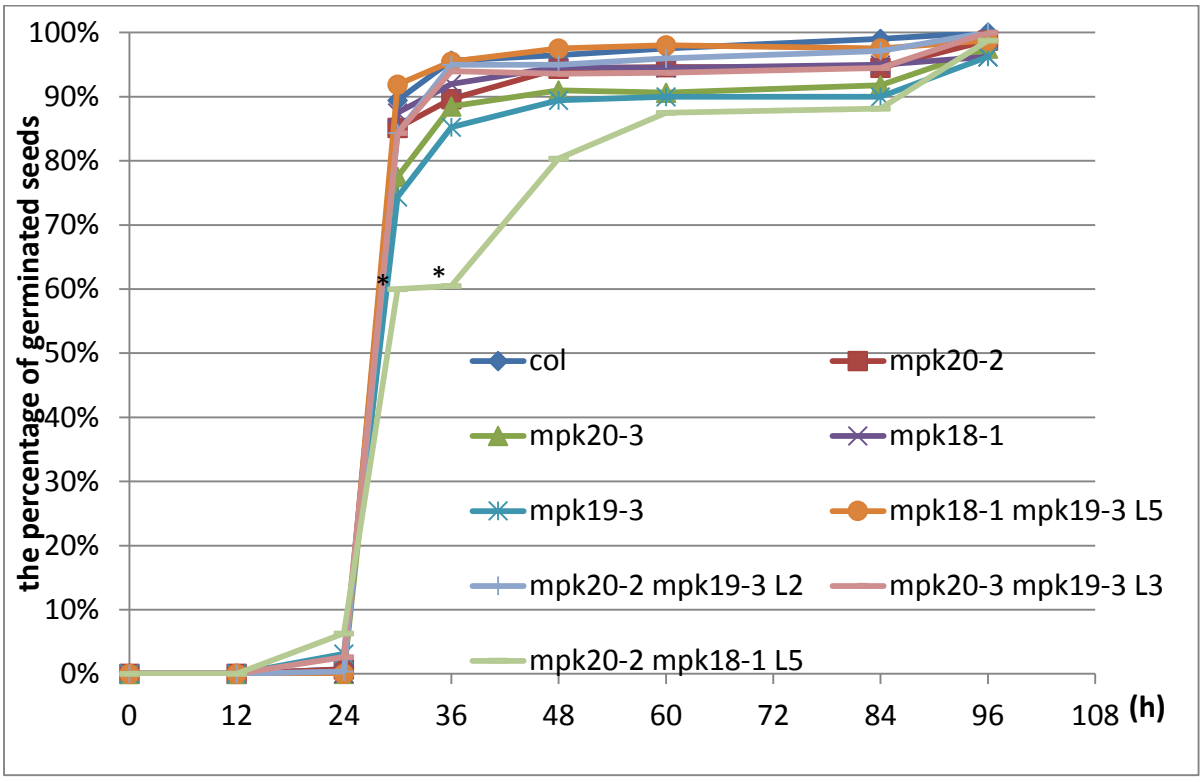


**Figure 3.9: The germination rates of Col 0 and *mpk18, 19, 20* single and double mutants at different time points.**

Three independent experiments were performed, and each time two 1/2MS petri dishes were each sown with 50 seeds from each line. All the seeds were stratified for 48 hours before transferring the plates to the growth room at 22-24 ℃ under 16h/8h photo-period. By t-test analysis (0.05 p value cut-off), only *mpk18-1 mpk20-2* germinated more slowly, whereas the other lines germinated simultaneously. The "*" mark indicates that the result is statistically different from the value for Col-0 seeds (by t test analysis, 0.05 p value cut-off).

As shown previously, *mpk20-2* seedlings have slightly shorter primary roots, and shorter hypocotyls when grown in the dark (Section 3.4 and 3.5). I therefore examined these two traits in all the double mutants, as well. The hypocotyl length was only measured in dark-grown 5d-old-seedlings, since both *mpk20*-2 and *mpk20*-3 seedlings were previously found to have shorter hypocotyls than Col-0 seedlings at that particular time point.

In this experiment, I found that all four single mutants had shorter hypocotyls compared with Col 0 (Figure 3.10). On the other hand, the hypocotyls of the *mpk20-3 mpk19-3* and *mpk20-2 mpk19-3* double mutants were not significantly different in length from each other, and both had hypocotyls that were longer than those of the single mutants. However, when compared with Col 0 hypocotyls, the *mpk20-3 mpk19-3* hypocotyl length was the same as Col 0, whereas *mpk20-2 mpk19-3* hypocotyls were significantly longer. This is similar to the situation I observed in the *mpk20 ko* mutant hypocotyl experiments, in that only *mpk20-2* shows significant differences in traits compared with Col 0, whereas *mpk20-3* behaves the same as wild type.

Wild-type hypocotyl length was observed in dark-grown *mpk18-1 mpk19-3* mutant seedlings as well, but *mpk20-2 mpk18-1* seedlings had shorter hypocotyls. However, this latter result might be caused by the slower germination observed in this double mutant (Figure 3.9). Therefore the true hypocotyl growth rate of *mpk20-2 mpk18-1* seedlings could differ less from the control than the present data might imply. A more detailed analysis of the hypocotyl growth patterns in Col0 and the mutants is shown in Figure 3.10b. These histograms show that Col-0 and three double mutants share same hypocotyl length distribution, whereas the hypocotyl length distribution of three single mutants is different from Col-0.

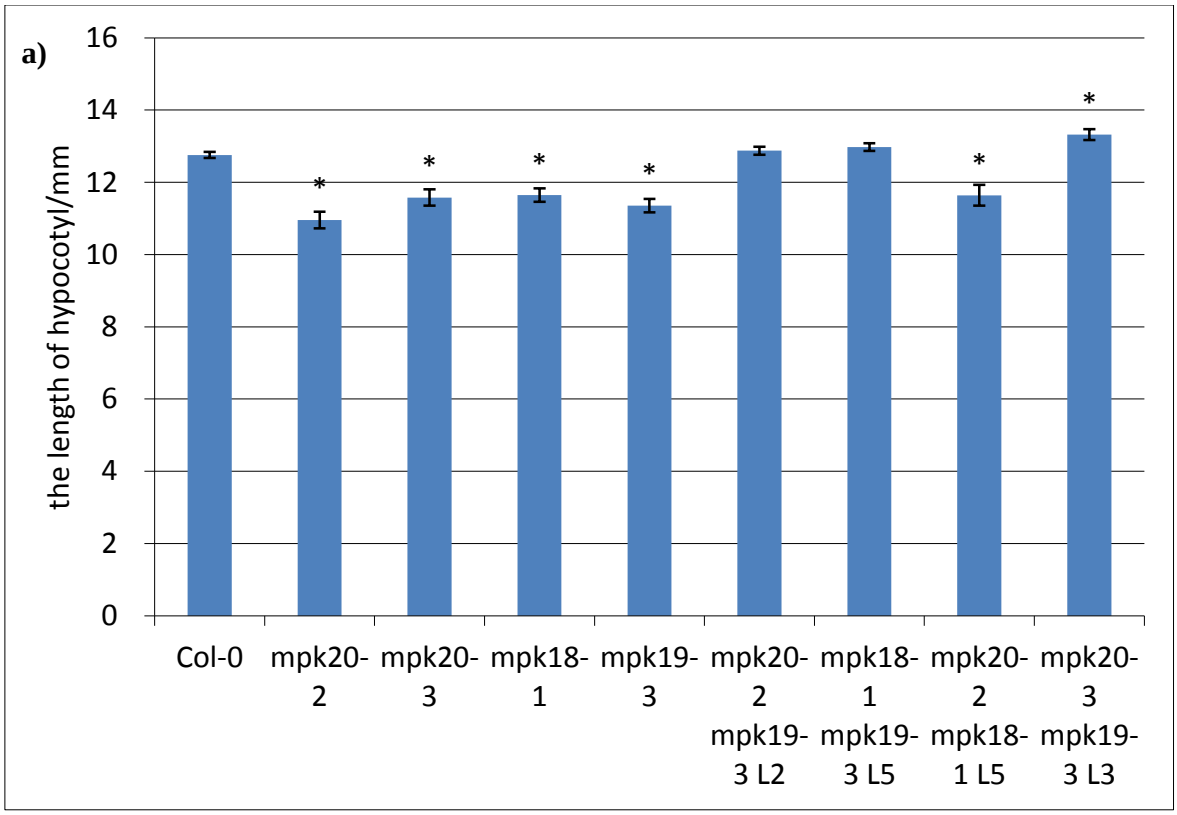
a)
the length of hypocotyl/mm
16
14
12
10
8
6
4
2
0
*
Col-0
mpk20-2
mpk20-3
mpk18-1
mpk19-3
mpk20-2 mpk19-3 L2
mpk18-1 mpk19-3 L5
mpk20-2 mpk18-1 L5
mpk20-3 mpk19-3 L3

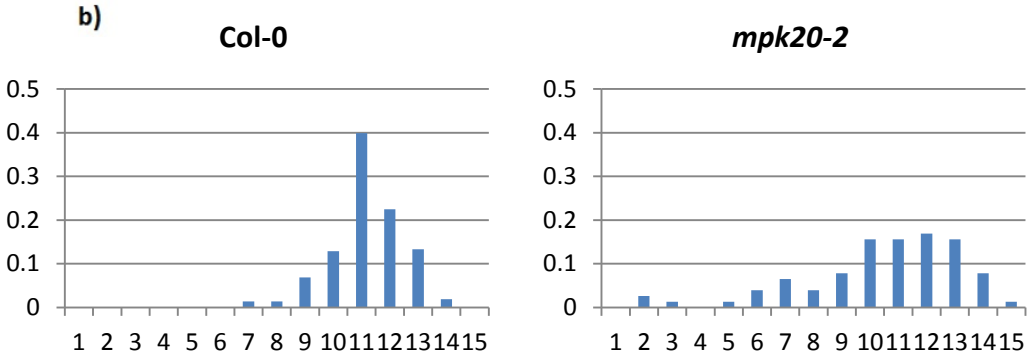
b)
Col-0
mpk20-2
0.5
0.4
0.3
0.2
0.1
0
1 2 3 4 5 6 7 8 9 10 11 12 13 14 15

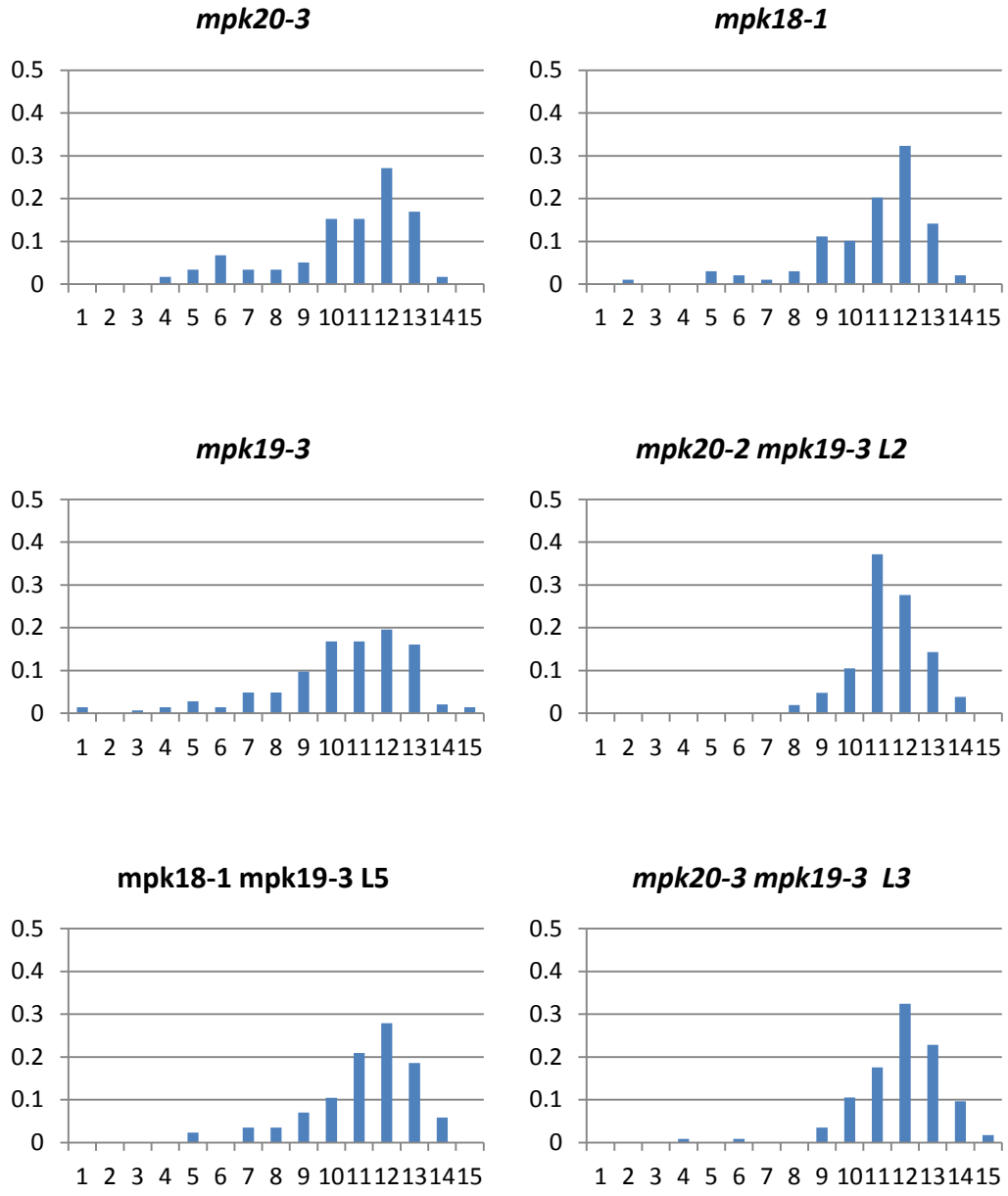


**Figure 3.10: Hypocotyl elongation of dark-grown seedlings of Col 0, *mpk18, 19* and *20 ko* mutants and their double mutants**

a) The length of 5-day-old dark-grown seedling hypocotyls. The labeling of *mpk20-2 mpk19-3 L2* refers to line 2 of the *mpk20-2 mpk19-3* double mutant. The "*" mark indicates that the result is statistically different from the value for Col-0 seeds (by t test analysis, 0.05 p value cut-off).

b) Histograms of hypocotyl length of the different lines. The Y axis represents the percentage of seedlings; the X axis represents the length of the hypocotyl.

The hypocotyl length of the seedlings was measured after growing in the dark for 5 days. The seedlings of Col 0, two single mutants and their double mutant were grown on the same Petri dish in order to create an identical growth environment. By t-test analysis, *mpk20-2*, *mpk20-3*, *mpk18-1*, *mpk19-3* and *mpk20-2 mpk18-1* seedlings have shorter hypocotyls, whereas *mpk20-3 mpk19-3* has longer hypocotyls, compared with Col 0. The data were collected from 120 seedlings of each line, from six independent experiments.

I next examined the primary root growth phenotype of the various mutant combinations. However, since these experiments were designed to test for possible functional redundancy, and *mpk20-3* seedlings had previously been shown to have the same root length as Col 0 seedlings (i.e. no phenotypic difference), the *mpk20-3* and *mpk20-3 mpk19-3* mutants were not included in this experiment.

I found that none of the *mpk18-1, mpk19-3,* or the *mpk18-1 mpk19-3* double mutant had a root elongation deficiency phenotype (Figure 3.11). This result would suggest that these two genes (*MPK18* and *19*) are not involved in primary root growth in *Arabidopsis* seedlings. Interestingly, however, *mpk20-2* seedlings were found to have shorter roots than either the *mpk20-2 mpk18-1* or *mpk20-2 mpk19-3* double mutants. In fact, *mpk20-2 mpk19-3* is the only mutant genotype whose root length was longer than that of Col 0. This apparent complementarity might indicate that the presence of MPK18 and/or MPK19 in *mpk20-2* plants results in a shorter root length phenotype, which in turn could mean that these three genes might all be participating in the root development process in Arabidopsis seedlings.

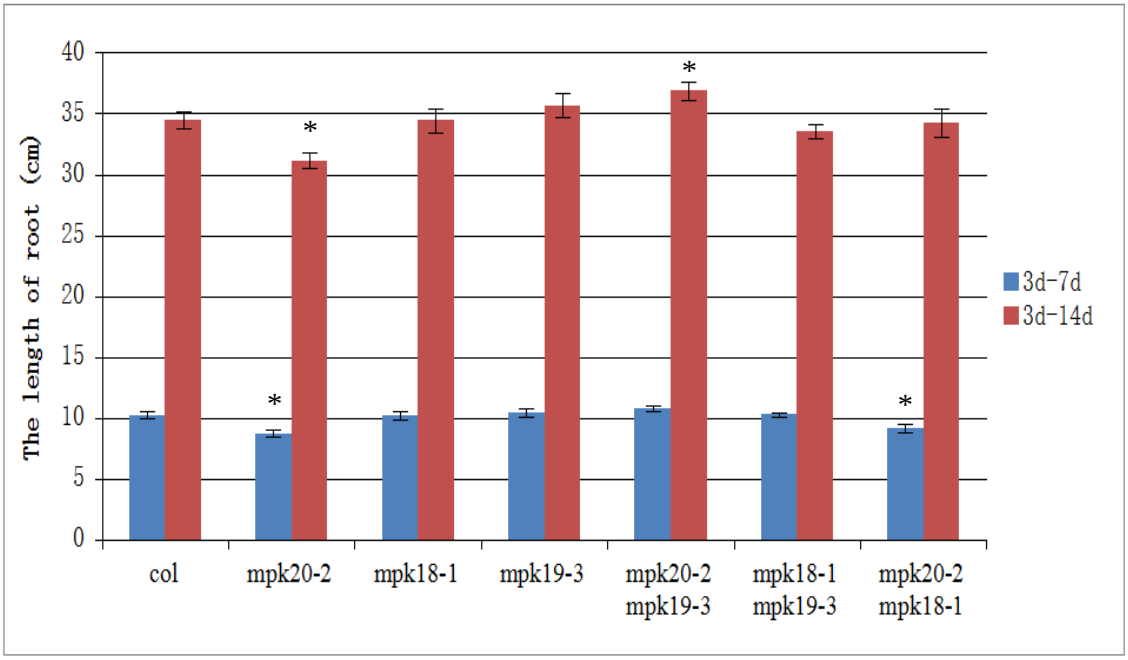


**Figure 3.11: The primary root elongation of Col 0, *mpk18, 19* and *20 ko* mutants and their double mutants.**

The root length was measured in six individual experiments using approximately 90 seeds from each line. Five seeds from Col 0, 5 seeds from single mutants (for instance *mpk20-2* and *mpk18-1*) and 15 seeds from each double mutant (for instance *mpk20-2 mpk18-1)* were planted on the same 1/2MS petri dish in each experiment. Compared with Col 0 root length, the root length of *mpk20-2* is shorter, whereas the others are basically the same as Col 0, except for *mpk20-2 mpk19-3*, which has slightly longer roots than Col-0. The "*" mark indicates that the result is statistically different from the value for Col-0 seeds (by t test analysis, 0.05 p value cut-off).

## 3.8 The phenotype of the triple mutant.

To help further evaluate whether functional redundancy might be obscuring deficiency phenotypes in the *mpk18*, *mpk19* and *mpk20* mutants, I crossed *mpk20-2 mpk19-3* plants with *mpk18-1 mpk19-3* plants and selected homozygous lines of the *mpk18 mpk19 mpk20* triple mutant from among the progeny for phenotype analysis. After genotyping and SQ RT-PCR, two triple mutant lines were identified and then analyzed: *mpk20-2 mpk18-1 mpk19-3* (L4) and *mpk20-2 mpk18-1 mpk19-3* (L6).

First, the germination rates of all three single mutants and the triple mutant lines were tested from 0h to 108h. Although the germination rates of the triple mutant lines were significantly lower than that of Col 0 up to the 60-hour time point, this difference disappeared after the 72-hour time point (Figure 3.12).

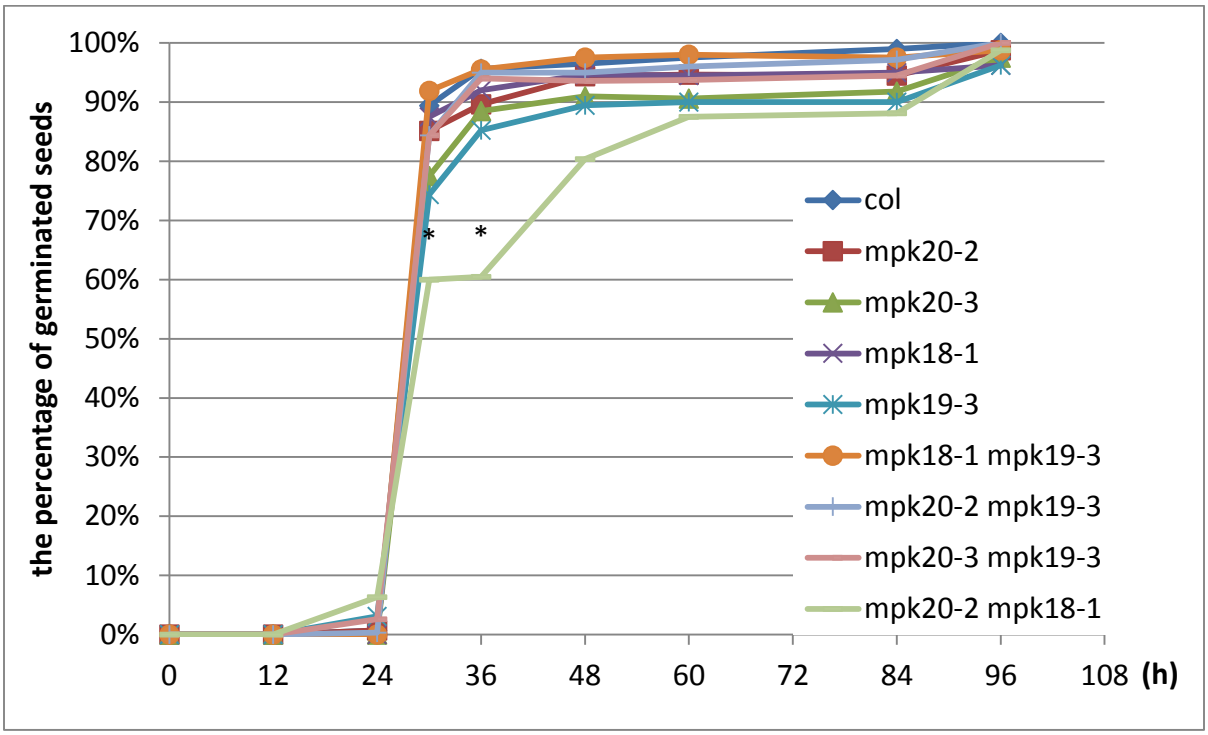


**Figure 3.12: The seed germination rate of Col 0 and various *mpk18, 19* and *20* mutants at different time points.**

Forty seeds from each line were planted on a 1/2MS Petri dish and stratified for 48 hours before being placed in germination conditions. Two dishes were used per experiment and two independent experiments were carried out. By t-test analysis (0.05 p value cut-off), at the 48-hour time point and 60-hour time point the germination rates of the two triple mutant lines (*mpk20-2 mpk18-1 mpk19-3 L4* and *mpk20-2 mpk18-1 mpk19-3 L6*) were lower than that of Col 0. The "*" mark indicates that the result is statistically different from the value for Col-0 seeds (by t test analysis, 0.05 p value cut-off).

Primary root extension in seedlings of two triple mutant lines was also reduced compared to that of Col-0, *mpk18-1*, or *mpk19-3* seedlings (Figure 3.13). Although the root length attained by 7-day-old triple mutant seedlings was shorter than that of *mpk20-2* seedlings, the primary root extension of 14-day-old *mpk20-2 mpk18-1 mpk19-3 L6* seedlings was the same as that of *mpk20-2* whereas *L4* roots were still shorter than those of *mpk20-2*. There is no statistically significant difference between the two triple mutants' root lengths at either time point.

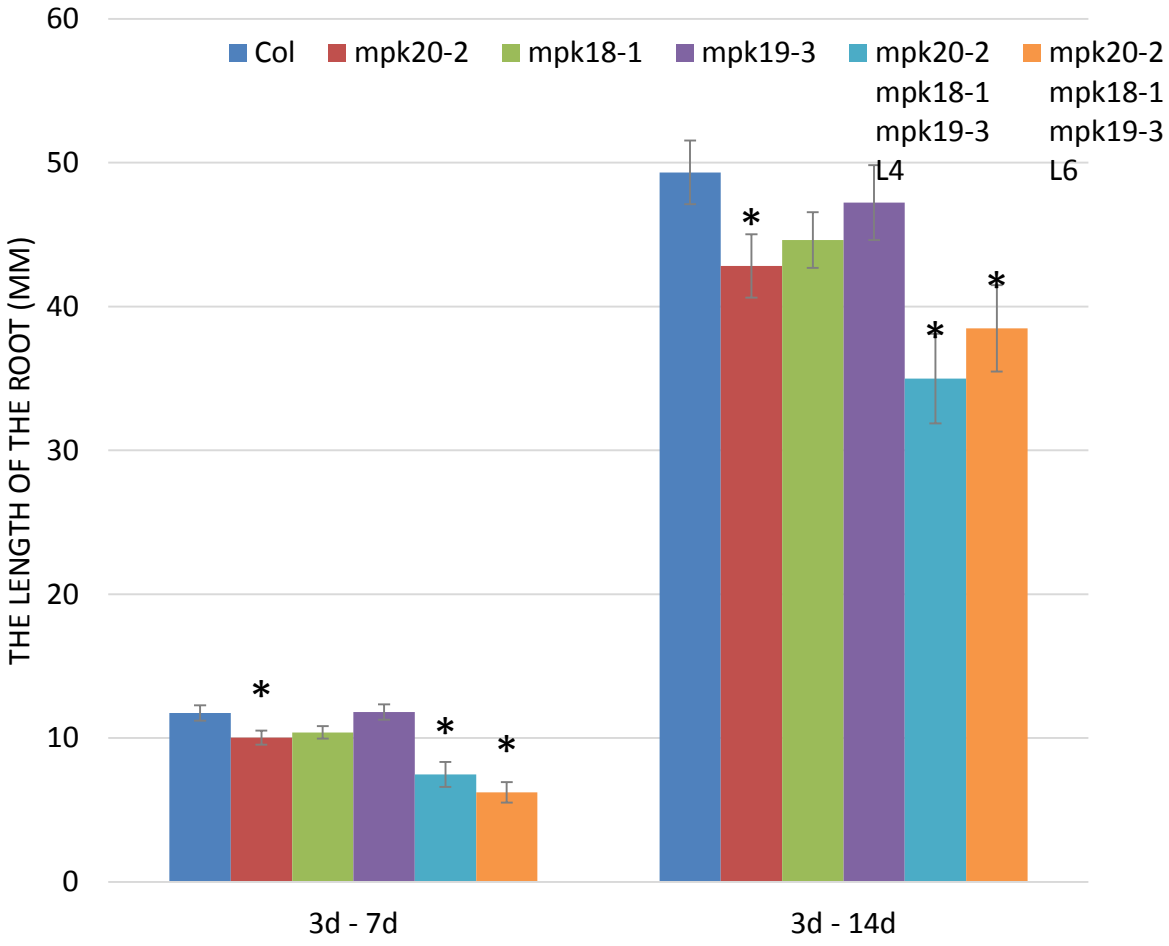


**Figure 3.13: The primary root growth of Col0 and *mpk18/19/20* triple mutants.**

The results were obtained from three experiments. In each experiment, two plates of seedlings were measured. Each plate contained 10 seeds from a triple mutant and 5 seeds from other lines. Since the

germination rates of the different lines were the same after the 72-hour time point, the length of root extension was measured from the 3-day growth point to the length achieved in 7-day-old or 14-day-old seedlings. The blue bars represent the root extension from the 3rd day till the 7th day, whereas the red bars show the root extension between the 3rd day and the 14th day. According to t-test analysis (0.05 p value cut-off), the root extension values for the *mpk20-2*, *mpk20-2 mpk18-1 mpk19-3 L4* and *mpk20-2 mpk18-1 mpk19-3 L6* mutants were significantly different from that of Col 0. The "*" mark indicates that the result is statistically different from the value for Col-0 seeds (by t test analysis, 0.05 p value cut-off).

## 3.9 Phenotype of *mpk20 ko* mutants under different hormone treatments.

According to the data in the MIND 0.5 database, derived from a survey using a mating-based split ubiquitin protein-protein interaction assay system, MPK20 interacts with PIN1. AtPIN1 helps regulate polar auxin transport in Arabidopsis, and auxin is known to inhibit primary root growth and stimulate lateral root formation [90]. In the context of my hypothesis that MPK20 is involved in primary cell wall synthesis or associated biochemical processes, this evidence for PIN1-MPK20 association led me to test the behavior of the *mpk20 ko* lines when treated with different IAA concentrations (Figure 3.14). Without auxin treatment, the primary root length of *mpk20-2* seedlings is shorter than that of Col 0, whereas the root length of *mpk20-3* is the same as that of Col 0. The root lengths of all three genotypes are reduced when the seedlings are grown in higher concentrations of IAA, but their relative growth responses are unaffected; i.e. the *mpk20* mutants respond in the same manner as Col 0 plants under different IAA treatment regimes.

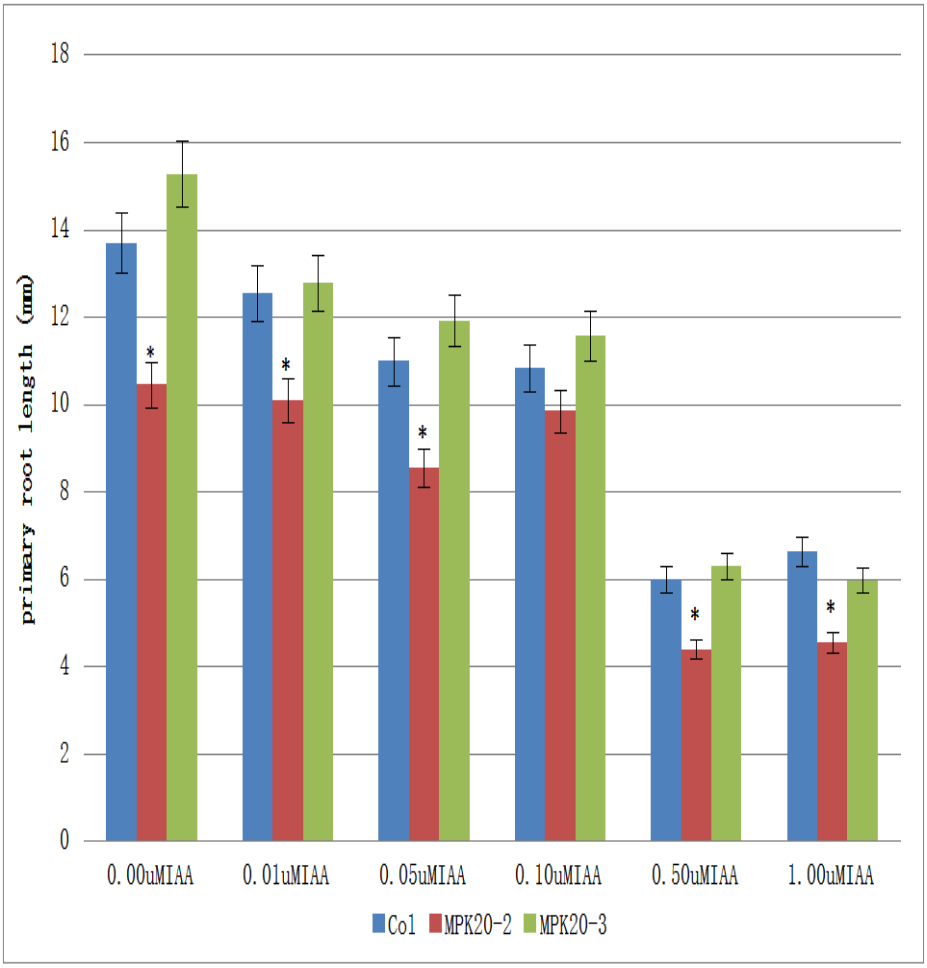


**Figure 3.14: The primary root growth of Col 0 and two *mpk20 ko* mutants in response to different concentrations of IAA.**

The root growth measurements were obtained from three independent experiments, each of which involved ~ 75 seeds from each genotype treated with each IAA concentration. The seeds were planted on 1/2MS plates, held in the dark at 4℃ for 48 hours and then grown under a 16h/8h photo-period at 22℃ for 2 days. The seedlings were then transplanted to 1/2MS plates supplemented with different concentrations of IAA. Since the IAA was dissolved in ethanol, the negative control 1/2MS+0.00μM IAA plates also contained 0.1% ethanol. The "*" mark indicates that the result is statistically different from the value for Col-0 seeds (by t test analysis, 0.05 p value cut-off).

Since PIN2 has been reported to act as a root gravitropism control protein [91], I next tested the gravity-response of *mpk20* mutant roots. When I rotated by 90 ° the growth plates on which seedlings of different genotypes were growing, I observed that *mpk20* mutants display the same growth response to this change in the gravity vector as did Col 0 seedlings, whereas the positive control *pin2 (eir1) ko* mutants showed a severe gravitropism deficiency phenotype both before and after the re-orientation of the plates (Figure 3.15).

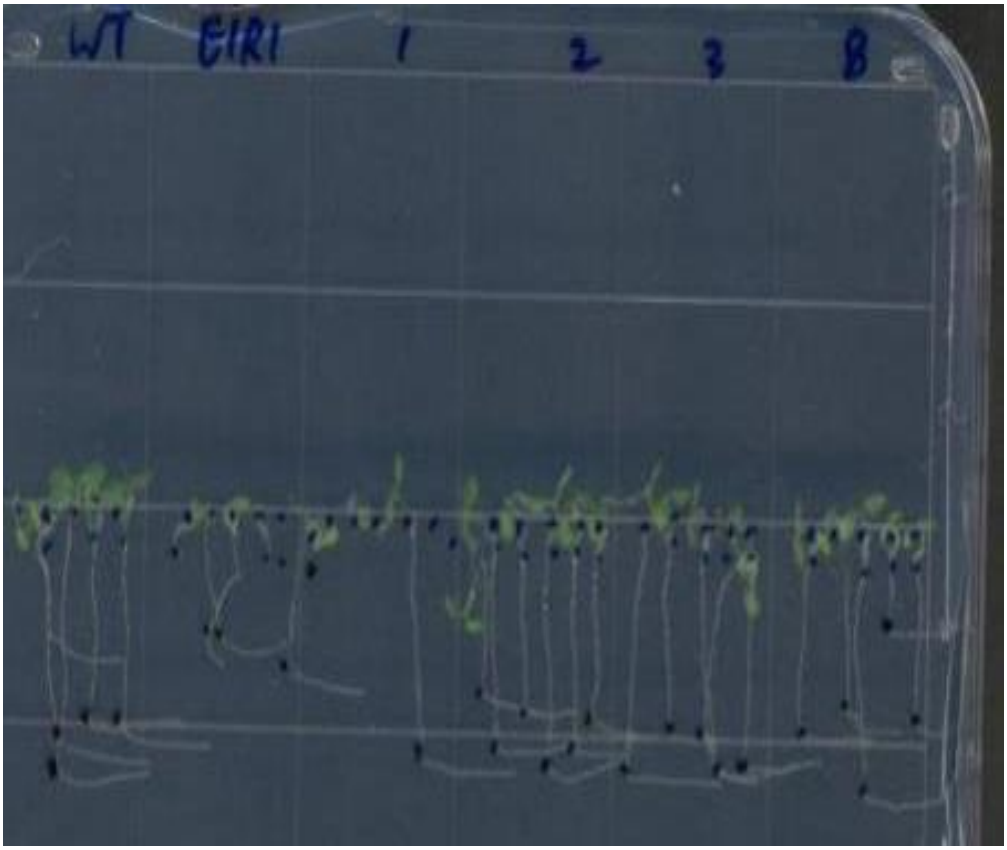


**Figure 3.15: The gravitropic response assay for *mpk20 ko* mutants.**

The seeds were stratified in the dark at 4℃ for 48 hours before being grown vertically at 22℃ under 16h/8h photo-period on 1/2MS plates. Two independent experiments were performed, and in each experiments one 1/2MS plate, containing five seeds from each line was assayed. After 6 days, the plates were turned clockwise 90°. "WT" represents the Col 0 seedlings, "EIR1" represents *pin2* seedlings, "1" represents *mpk20-1* mutant, "2" represents *mpk20-2* mutants, "3" represents *mpk20-3* mutant, and "8"

represents *mpk18-1* mutants. The positive control *pin2* seedlings display a gravitropism deficiency phenotype before and after turning the plate, while other mutants behave the same as Col 0.

Since high concentrations of either 2,4-D (2,4-dichlorophenoxyacetic acid) or IAA inhibit the expansion of the cotyledon [92-94], a process that requires cell wall synthesis/extension, the cotyledon expansion of *mpk20 ko* mutants was measured and compared with that of Col 0 seedlings. The cotyledons of *mpk20-2* seedlings are already smaller than those of either Col 0 or *mpk20-3* after growing on 1/2MS plates for 5 days (Figure 3.16a). At that point, half of the seedlings were moved from 1/2MS plates to 1/2MS plates with additional IAA or 2,4-D. By t test (0.05 p value cut-off), the cotyledon expansion of Col 0 and *mpk20-3* is significantly inhibited by treatment with IAA, whereas expansion of *mpk20-2* cotyledons is unaffected (Figure 3.16b). In response to exogenous 2,4-D treatment, cotyledon expansion of both Col 0 and the two *mpk20 ko* mutants was inhibited to a similar degree (Figure 3.16c).

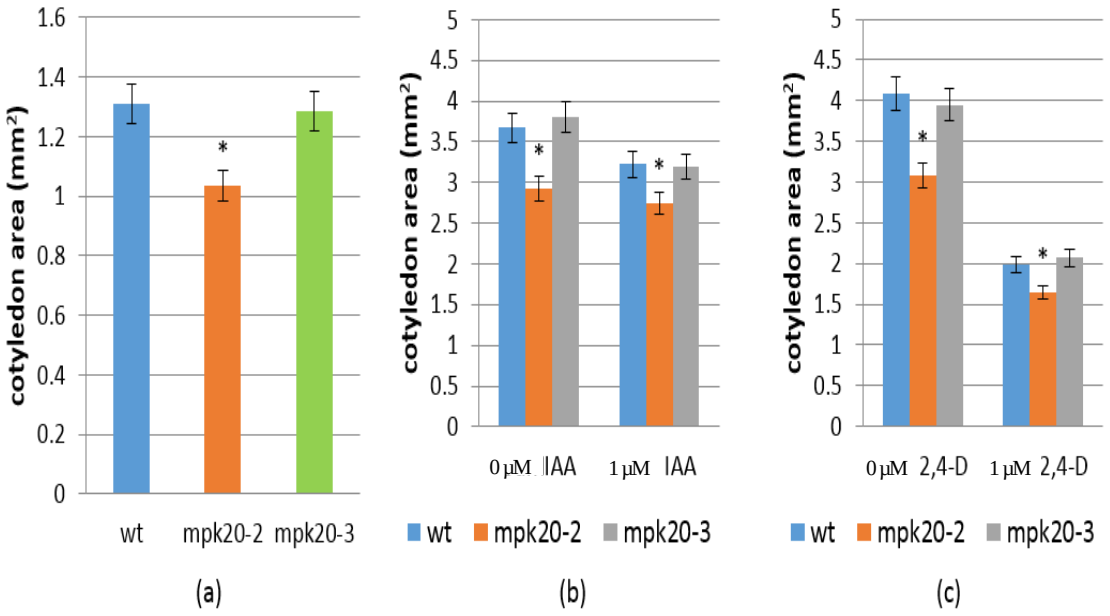


**Figure 3.16: The cotyledon expansion of Col 0 and *mpk20 ko* mutants in response to different concentrations of IAA or 2,4-D.**

a) The seeds were planted on 1/2MS plates, stratified at 4℃ for 48 hours and grown in 22℃ under 16h/8h photoperiod for 5 days. The cotyledons were photographed and the cotyledon area was measured by using Image J software. The data were collected from three independent experiments each of which contained 120 seedlings from each genotype. The "*" mark indicates that the result is statistically different from the value for Col-0 seeds (by t test analysis, 0.05 p value cut-off).

b) After 5 days growth on 1/2MS, the seedlings were transplanted to 1/2MS + 0μM IAA (containing 0.1% ethanol) or 1/2MS + 1μM IAA. Three independent experiments were performed. The results show the average cotyledon area of 30 seedlings each from Col 0 plants and *mpk20 ko* mutants under different concentration of IAA. The "*" mark indicates that the result is statistically different from the value for Col-0 seeds (by t test analysis, 0.05 p value cut-off).

c) After 5 days growth on 1/2MS, the seedlings were transplanted to 1/2MS + 0.1% ethanol or 1/2MS + 1μM 2,4-D. The graphs show the cotyledon area of 30 seedlings of each line as assessed in three independent experiments. The "*" mark indicates that the result is statistically different from the value for Col-0 seeds (by t test analysis, 0.05 p value cut-off).

It has been reported that not only the homeostasis but also the crosstalk of phytohormones is important in MPK-regulated plant development, stress response and disease resistance [95-97]. Therefore, the responsiveness of the *mpk20* mutants to other exogenous hormone conditions was also examined.

1-Aminocyclopropane-1-carboxylic acid (ACC) is an ethylene precursor [98], and when exogenous ACC is added to growth media it effectively mimics endogenous ethylene production. It has been reported that application of ACC inhibits hypocotyl elongation in dark-grown seedlings of Arabidopsis [99, 100]. Application of brassinazole (BRZ), a brassinosteroid biosynthesis inhibitor, also leads to shorter etiolated hypocotyls in Arabidopsis [101]. When I examined the response of dark-grown wild type and *mpk20* mutant seedlings to ACC and BRZ application, I found that while hypocotyl extension of Col 0 and the two *mpk20* mutants is reduced by these treatments, there is no obvious difference in the response of the *mpk20* mutants, relative to the Col 0 response (Figure 3.17 & Figure 3.18).

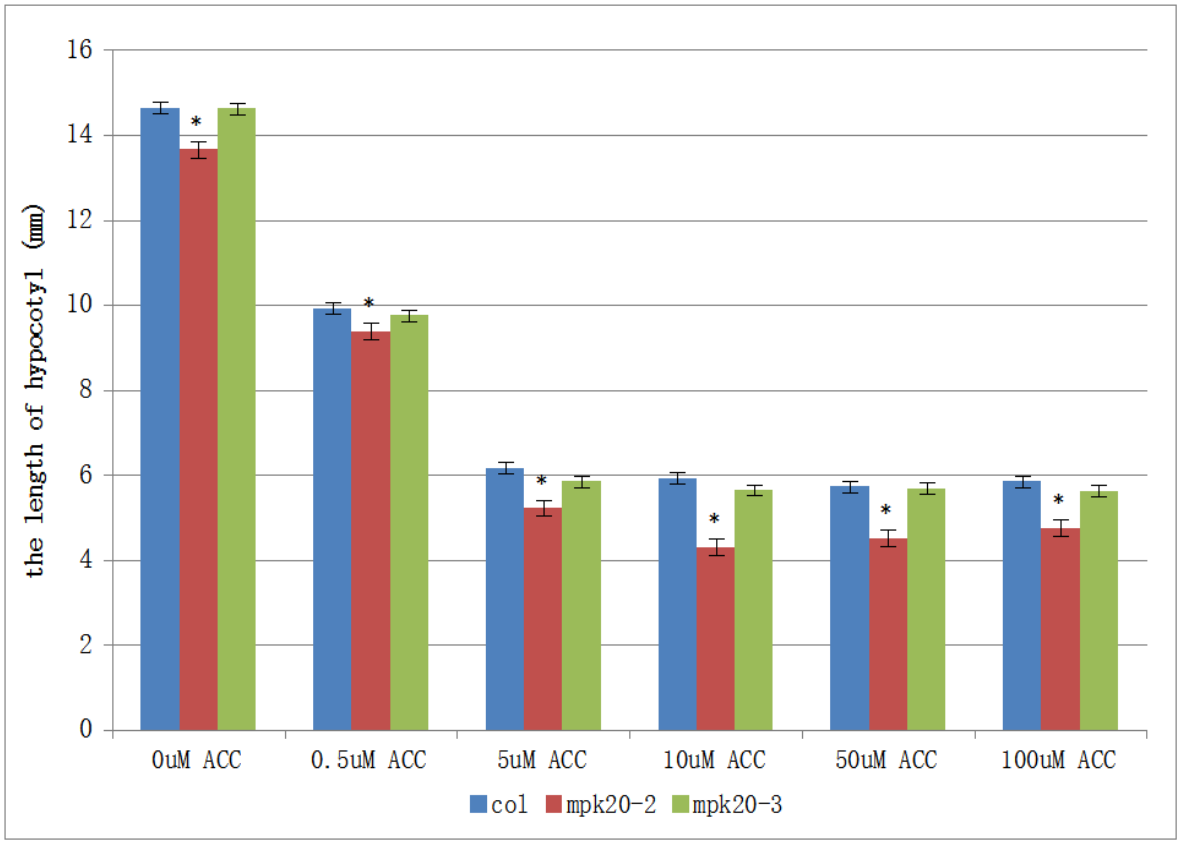


**Figure 3.17: Hypocotyl elongation of Col-0 and *mpk20 ko* mutants in response to different concentrations of ACC.**

The seeds of the different genotypes were planted on 1/2MS plates, stratified at 4℃ for 48 hours, and then grown in 22℃ for 1 day under a 16h/8h photo-period. They were then transplanted to ½ MS plates supplemented with different concentrations of ACC and grown in the dark for 5 days. The negative control (1/2MS + 0μM ACC) contained 0.1% ethanol, since the ACC was dissolved in ethanol. The data were collected from four independent experiments and each bar represents the average hypocotyl length for approximately 80 seeds. The "*" mark indicates that the result is statistically different from the value for Col-0 seeds (by t test analysis, 0.05 p value cut-off).

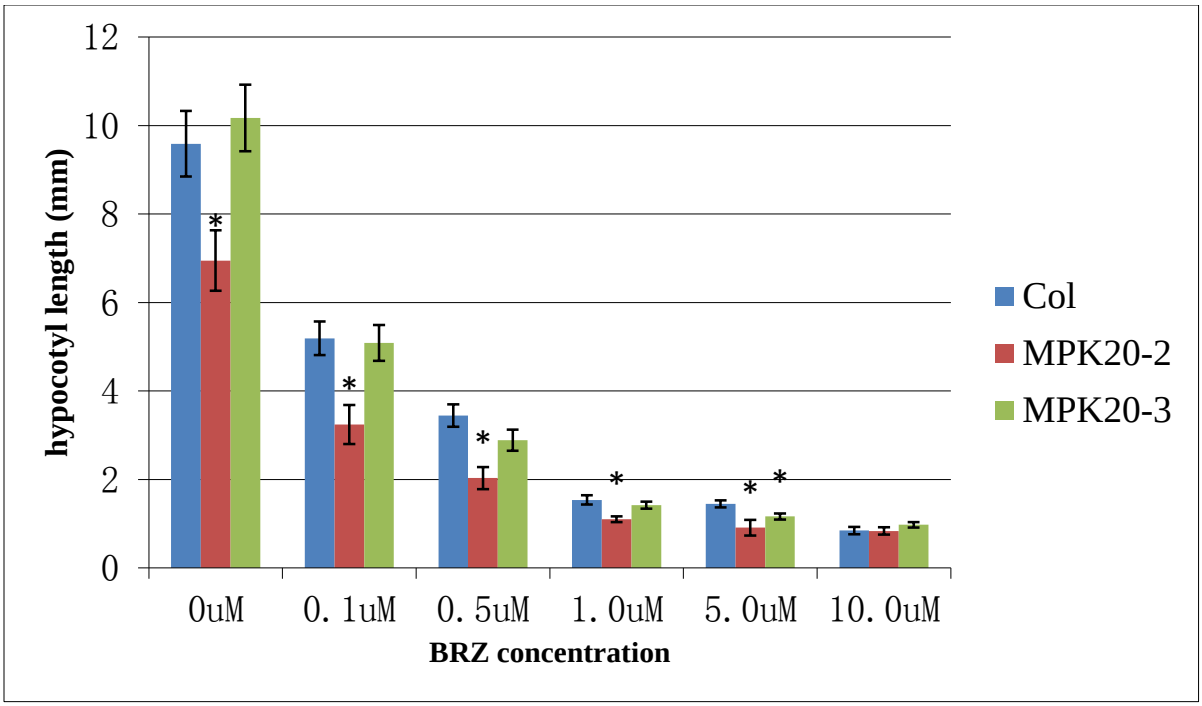


**Figure 3.18: The hypocotyl elongation of Col-0 and *mpk20 ko* mutants in response to different concentrations of BRZ.**

The seeds were stratified at 4℃ for 48 hours on 1/2MS plates, grown at 22℃ for 1 day under 16h/8h photo-period, and then were transplanted to1/2 MS plates supplemented with different concentrations of BRZ and grown tilted in the dark for 5 days. The blank control group was grown on 1/2MS plates containing 1% dimethyl sulfoxide (DMSO), since the BRZ was dissolved in DMSO. Two independent experiments were performed and 30 seedlings were measured for each line at each BRZ concentration. The "*" mark indicates that the result is statistically different from the value for Col-0 seeds (by t test analysis, 0.05 p value cut-off).

Another hormone that has been implicated in cell wall formation is gibberellic acid (GA), which acts through a family of signaling proteins called DELLA proteins. RGA (REPRESSOR OF ga1-3) is one such DELLA protein. Plants transformed with a GFP–tagged form of RGA (*pRGA:GFP-RGA*) display a fluorescent signal in their root cell nuclei, and this signal rapidly disappears after treating the plants with exogenous GA [102], indicating that GA can induce the destabilization of RGA. However, if the *pRGA:GFP-RGA* plants are also expressing an *AtPIN1*-

*RNAi* construct they show no GA-mediated disappearance of GFP-RGA. This result suggests that AtPIN1 (or associated auxin transport patterns) promote the disappearance of RGA when GA concentrations rise in the plants [102]. Bearing in mind the predicted association of MPK20 with PIN1, I wanted to test the responsiveness of the *mpk20* mutants to GA. The hypocotyl elongation of Col 0 and the two *mpk20 ko* mutants was therefore measured in dark growth conditions in the presence of either exogenous $GA_3$ or paclobutrazol (PAC), which is a GA biosynthesis inhibitor [42]. The hypocotyl length of Col-0 seedlings increased 5% on GA plates, relative to untreated seedlings, and decreased 66% on PAC plates. In comparison, the hypocotyl length of *mpk20-2* seedlings increased 15% on GA plates, relative to the untreated seedlings, and decreased 62% on PAC plates. The *mpk20-3* seedlings, however, behaved similarly to Col-0 seedlings, with a 7% increase in hypocotyl length in response to GA and a 63% reduction in extension in response to PAC treatment (Figure 3.19).

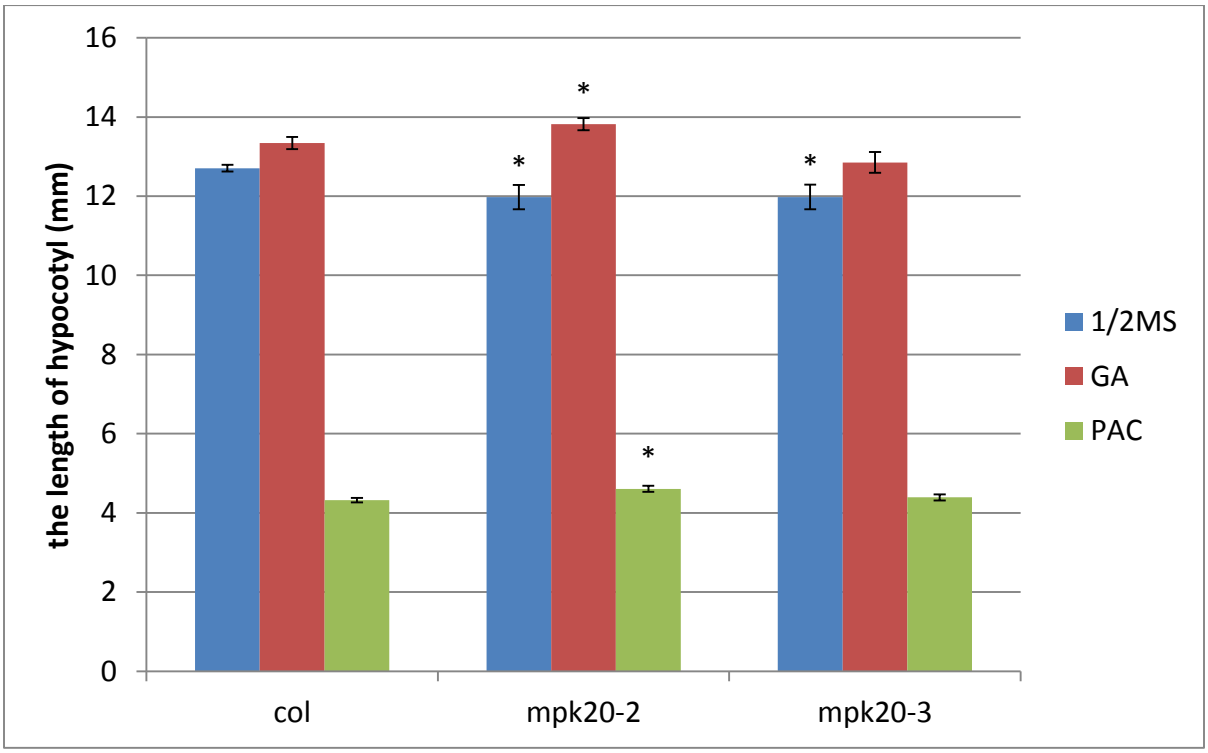


**Figure 3.19: Hypocotyl elongation of dark-grown Col 0 and *mpk20 ko* mutants treated with 10µM $GA_3$ or 1µM PAC.**

The seeds were planted on 1/2MS plates, stratified at 4℃ for 48 hours, and grown at 22℃ for 1 day under a 16h/8h photo-period. They were then transplanted to 1/2MS plates, 1/2MS + 10 μM $GA_3$ plates or 1/2MS + 1 μM PAC plates, and held in dark for 5 days. The control 1/2MS plates contained 0.1% ethanol, as the PAC was dissolved in ethanol. The "*" mark indicates that the result is statistically different from the value for Col-0 seeds (by t test analysis, 0.05 p value cut-off).

### 3.10 Purification of recombinant MPK20 protein

In order to test the ability of MPK20 to phosphorylate possible target proteins *in vitro*, such as PIN1, I tried to prepare a recombinant version of the kinase by expressing a chimeric *MPK20-GST* construct in *E. coli*. The cDNA of *MPK20* was first cloned into three different bacterial expression vectors: pGEX4T-1, pET-28 and pEXP1-DEST, and these constructs were transformed into One Shot® BL21 (DE3) *E. coli* cells. Despite adjusting the IPTG (isopropyl β-D-1-thiogalactopyranoside) inducer concentration (0.1 μM, 0.25 μM, 0.5 μM, 0.75 μM, or 1.0 μM), the incubation temperature (16° C, 22° C, or 37° C) and the period of induction (2h, 5h, or 16h), no convincing evidence of induction of MPK20 expression could be obtained when examining the bacterial protein extracts on PAGE gels and staining with Coomassie Blue (Figure 3.19).

I also attempted to obtain transient ectopic expression of GFP or RFP-tagged MPK20 *in planta* by infiltrating leaves of *Nicotiana benthamiana* with the *MPK20* cDNA cloned into either the pEG102, pEG103 or pEG203 vectors. No GFP/RFP signal was observed in the infiltrated leaf tissue when examined by confocal microscopy. In addition, Dr. A. Tauxin was unable to obtain expression of MPK20 protein in the *Pichia* yeast expression system (co-operative work with Dr. Tauxin in Dr. Harry Brumer's laboratory, MSL).

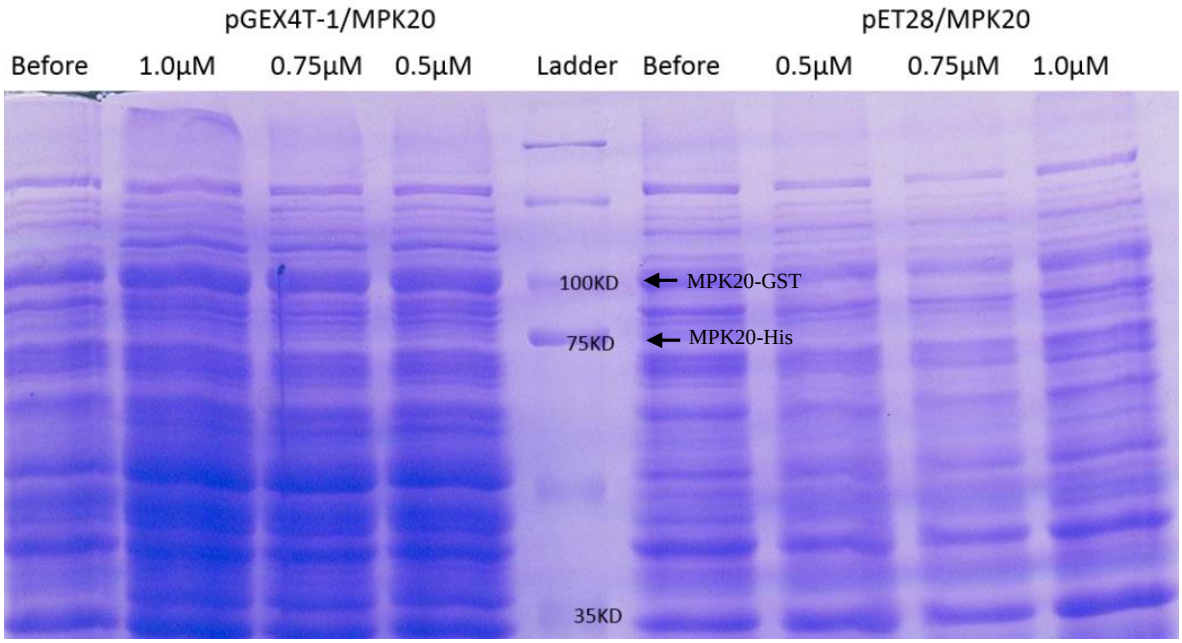


**Figure 3.20: No induction of MPK20-GST or MPK20-His$_3$ accumulation could be detected in bacterial cells after adding IPTG and fractionating the cell extracts by PAGE and Coomassie Blue staining.**

The bacterial cultures were harvested after 16 hours IPTG incubation in 22℃. The MPK20 predicted molecular mass is 69KD, therefore MPK20-GST in pGEX4T-1/MPK20 should run around 95KD, whereas the MPK20-His in pET28/MPK20 should be around 69KD. "Before" represent the expressed proteins detected before adding IPTG, "1.0μM" represents adding 1.0μM IPTG, "0.75μM" represents adding 0.75μM IPTG, and "0.5μM" represents adding 0.5μM IPTG.

# 4 Discussion

## 4.1 Role of MPK20 in hypocotyl and root elongation in Arabidopsis seedlings

Previous studies led me to hypothesize that MPK20 might be somehow involved in primary cell wall metabolism. For instance, *MPK20* is co-expressed with primary cell wall cellulose synthases CesA1, 3 and 6 [62], and the expression of *CesA1* is directly correlated with *MPK20* expression in the ATTED co-expression database [77, 79]. To test this hypothesis, I conducted a reverse genetics analysis of *MPK20*, and of some of its most closely related homologues within the Group D MPKs, focusing on traits related to plant primary cell wall biosynthesis.

For the reverse genetics analysis, I was initially able to obtain three *mpk20 ko* mutants (*mpk20-1*, *mpk20-2* and *mpk20-3*) that could potentially be loss-of-function alleles. I found that the dark-grown *mpk20-2* mutant hypocotyl is approximately 15% shorter than the Col 0 plant hypocotyl, whereas the *mpk20-3* mutant hypocotyl is approximately 10% shorter than Col 0 (Figure 3.5). When comparing primary root elongation rates among the mutants and Col 0 plants, the *mpk20-2* root is about 10% shorter than the Col 0 root in my assays, whereas the *mpk20-3* root is essentially the same as that of Col 0 (Figure 3.6). These results suggest that, although both *mpk20-2* and *mpk20-3* plants lack *MPK20* transcripts, the *mpk20-2* genotype shows a stronger deficit in primary cell wall elongation.

There are two possible explanations for this pattern of allele-specific responses; one is that knocking out *MPK20* in *Arabidopsis* has no effect on plant growth, whereas one or more other T-DNA insertions in the *mpk20-2* genome could be resulting in decreased hypocotyl elongation. Another possibility is that the T-DNA insertion in *MPK20* locus does affect elongation, but possible additional T-DNA insertions in one or both *ko* mutants are having counteracting effects that influence the outcome of the *MPK20* insertion.

The magnitude of the apparent growth deficiency observed in the *mpk20* mutants is small. It has been reported, for example, that the dark-grown *prc1* mutant (*CesA6 ko* mutant) hypocotyl is 75% shorter than the Col 0 hypocotyl, while its root length is about 50% shorter than Col 0 [76]. In

contrast, the *mpk20 ko* mutants in my study do not show a similar magnitude difference in either hypocotyl extension or root extension growth. This might indicate that MPK20 does not play a central role in these tissue elongation processes. On the other hand, since *MPK20* has two close paralogues, *MPK18* and *MPK19*, the redundant function of these three proteins might be suppressing the effect of losing *MPK20* in Arabidopsis. Therefore the various double knock out mutants and the triple knock out mutant of *MPK18*, *MPK19* and *MPK20* were generated and examined.

If functional redundancy between some or all of these paralogous genes is suppressing the loss-of-function phenotype of *mpk20* seedlings, I would anticipate that a more severe phenotype would appear in the double/triple mutant genotypes. Instead, when I measured the hypocotyl extension in dark-grown seedlings of *mpk20*, *mpk18*, *mpk19* and their double mutants (Figure 3.10), I observed that, while all the single mutants have a shorter hypocotyl than the Col 0 seedlings, the hypocotyls of the various double mutants are as long as those of Col 0 plants. I can propose two models to address this apparent contradiction, as follows. Note that, since the *mpk20 mpk18* double mutant seems to germinate later than the other genotypes (Figure 3.9), this growth delay is likely to have affected the measurement of hypocotyl elongation in this double mutant. Comparison of hypocotyl extension in *mpk20 mpk18* double mutant with other genotypes is therefore not justified at this point, and I have excluded MPK18 from my models.

My first model hypothesizes that putative substrate X is needed for cell elongation, and the un-phosphorylated form of X has substantial basal activity (which we can call 100%) (Figure 4.2a). If substrate X is phosphorylated on site ‘A’ by MPK20, this results in a modest increase in its activity/function. This would be the situation for the WT plant, and we can call this slightly enhanced activity of substrate X 120%. The *mpk20-2* plants will therefore have only basal activity of the putative substrate X (i.e. 100%).

If phospho-substrate X is phosphorylated on a second site (‘B’) by MPK19, this counteracts the stimulatory effect of site ‘A’ phosphorylation by MPK20, and returns the doubly phospho-substrate X to a basal activity state (~100%).

If MPK19 is absent (in the *mpk19 ko* lines) and MPK20 is present, substrate X will have 120% activity. If MPK20 and 19 are both absent, the substrate should have 100% activity.

Another possibility is that the two MPKs each target different substrates (A and B), each of which inhibits hypocotyl elongation through a separate mechanism, but which interact with each other as phospho-forms to form a non-functional P-A + P-B complex. In this scenario, normal hypocotyl extension results when this non-functional complex is present. Therefore, when knocking out both MPKs, the levels of the two non-phosphorylated substrates both increase, which leads to a normal hypocotyl extension. When we knock out only MPK20, the amount of its substrate (A) increases. This results in MPK19's substrate (B) only being able to form a non-functional complex with part of the pool of A, while the remaining A continues to function as a hypocotyl elongation inhibitor, which leads to a shorter hypocotyl. (Figure 4.2b).

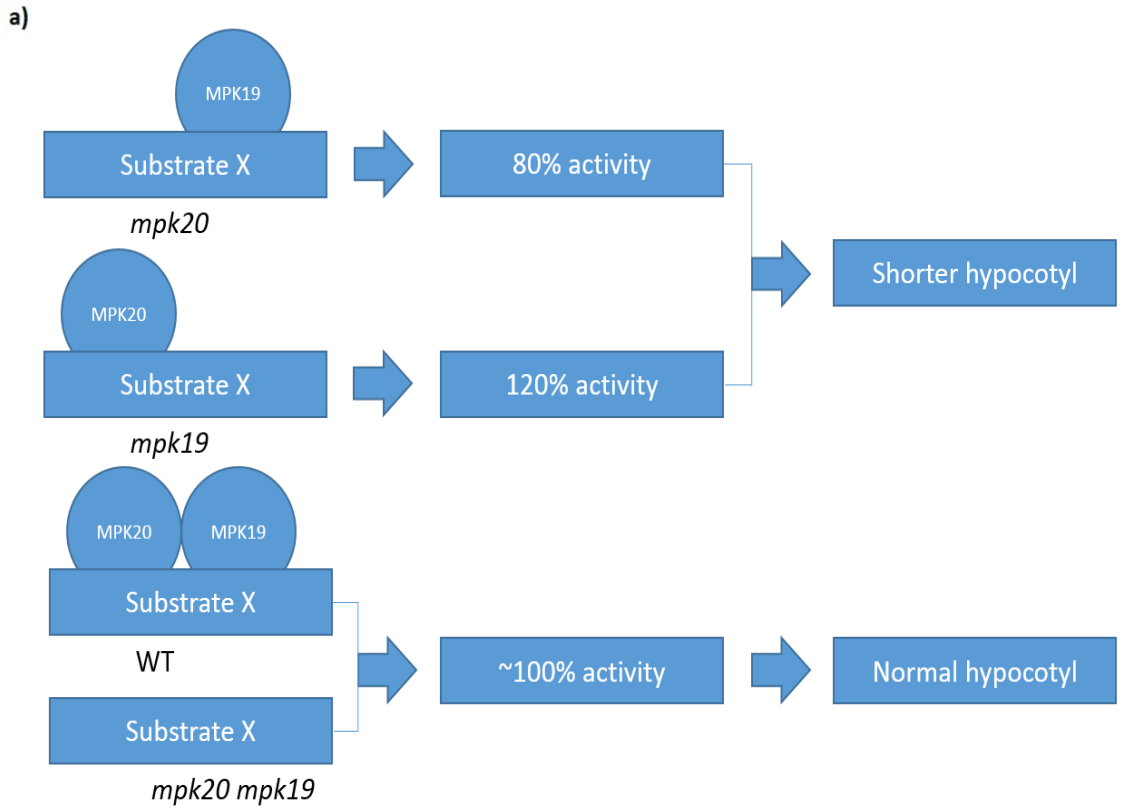

b)

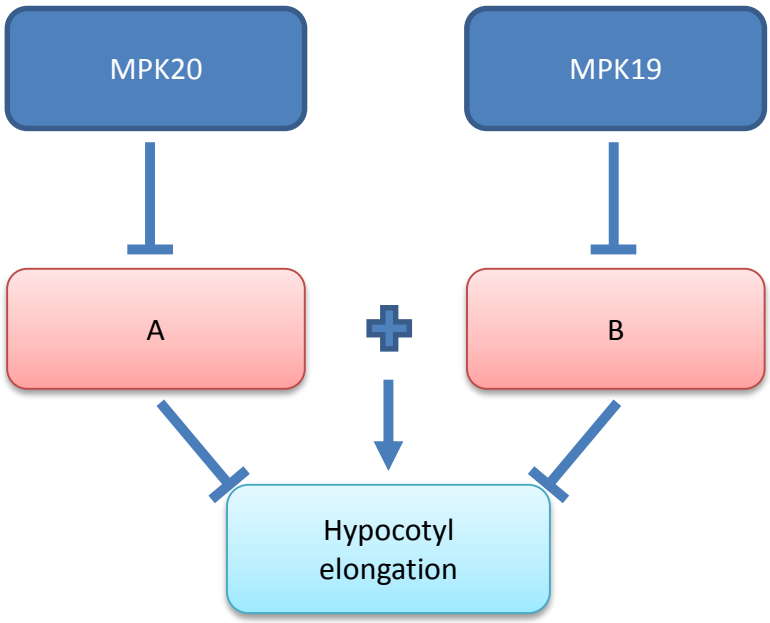


**Figure 4.1: Two models of possible relationships between MPK19 and MPK20 in hypocotyl elongation process.**

In the primary root growth experiment, *mpk18-1*, *mpk19-3*, *mpk18 mpk19*, *mpk20-2 mpk18* and *mpk20-2 mpk19* mutant all have normal root lengths, while *mpk20-2* has shorter root length than Col plants. Compared with the root length of *mpk20-2*, the roots of *mpk20-2 mpk18-1* and *mpk20-2 mpk19-3* are statistically longer. It seems that the absence of MPK18 or MPK19 increases the root length of *mpk20-2*. The possible explanations are that MPK20 may inhibit the upstream activator(s) of MPK18/MPK19, or may directly inhibit MPK18/MPK19, one or both of which normally act as a negative regulator in the root elongation process. Neither the *mpk18* nor *mpk19 ko* mutant has a shorter root than Col 0, however, although this might reflect the redundant function of these two MPKs. The *mpk18 mpk19* double mutant should be built and examined in the future for more clues.

Later, I found that the root of *mpk18 mpk19 mpk20* triple ko mutant is shorter than the Col root, and is even shorter than the *mpk20-2* root (about 65% of the Col root length). This suggests that the presence of MPK18 and MPK19 in the *mpk20 ko* mutant still contributes to root growth. Therefore my model should be altered as shown in figure 4.2. In Col 0 plants, the root elongation

pathway is positively regulated mainly by MPK20 and partly by MPK18/19. In addition, the activities/functions of MPK18 and MPK19 are suppressed by MPK20 in this pathway. Therefore, the root elongation pathway in *mpk18* or *mpk19 ko* mutants is still regulated by MPK20 which results in normal root length. In the *mpk20 ko* mutant, the MPK18/MPK19-related root elongation pathway is no longer inhibited by MPK20 and partly rescues the phenotype of shortened roots. To test this hypothesis, we could re-transform the triple mutant with a *MPK20* over-expression construct (e.g. *35S::MPK20*) and to see whether the root of the resulting plant is longer than the Col 0 root.

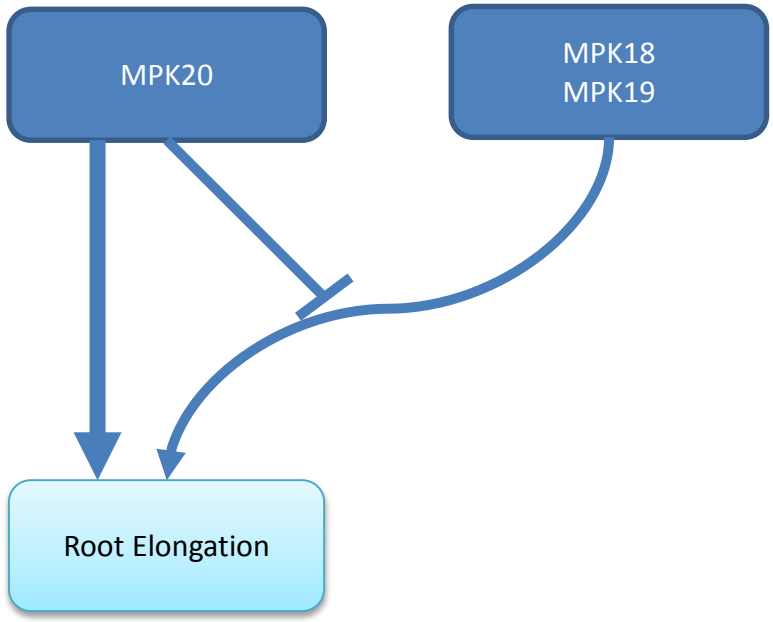


**Figure 4.2: A model for the possible relationship of the three MPKs (MPK18, 19 and 20) in the primary root growth process.**

It is possible that MPK20 is capable of directly phosphorylating MPK18 and MPK19, since multiple MPK phosphorylation motifs (T/SP) are observed when the three MPK protein sequences are aligned, as shown in Figure 4.3. Moreover, in the AtPIN (*Arabidopsis thaliana* protein interaction network) database, MPK18 is predicted to interact with MPK20 [103].

However, further experiments, such as *in vitro* kinase assays with recombinant proteins, would be necessary to strengthen these suggested models.

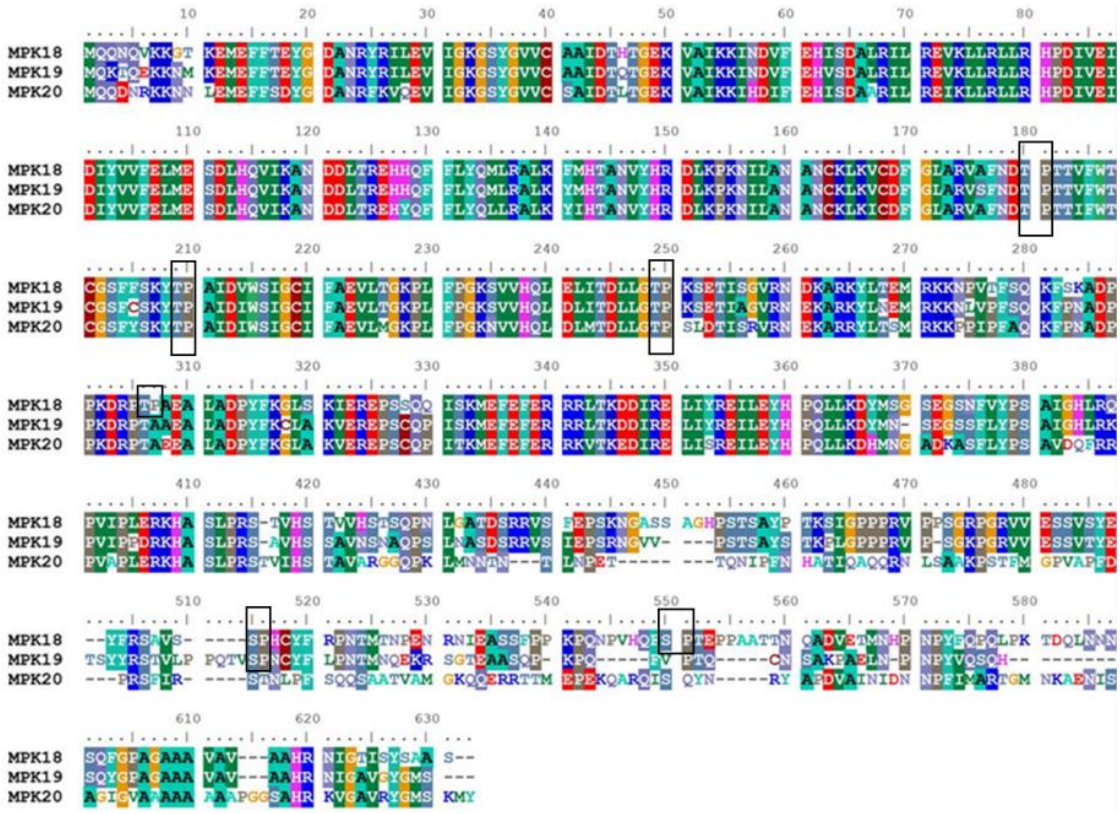


**Figure 4.3: The alignment of MPK18, MPK19 and MPK20 protein sequences (analysis by Clustal X). The black boxes show the possible MPK phosphorylation sites.**

## 4.2 MPK20 as a negative regulator in a GA signaling pathway

As several MPKs are involved in phytohormone signaling, and AtPIN1 is predicted to serve as a potential substrate for MPK20, the behavior of *mpk20* mutants when treated with different plant hormones was examined, but the only suggestion of a potential role for MPK20 in hormone responses was found in the context of GA signaling.

The hypocotyl of etiolated *mpk20-2* seedlings is shorter than that of Col 0 (WT) seedlings on 1/2MS plates, but longer than WT on 1/2MS+$GA_3$ plates and 1/2MS+PAC (a GA biosynthesis inhibitor) plates (Figure 3.18). In *mpk20-2* and *mpk20-3*, the percentage increase in hypocotyl elongation induced by adding $GA_3$ is less than the increased amount of Col. In the meanwhile, the PAC-induced reduction in *mpk20 ko* mutants root length is less than that of Col 0. Thus, *mpk20 ko* mutants seem more sensitive to GA3 than Col 0 seedlings. It should be mentioned that the change in hypocotyl elongation in *mpk20-3* in response to altered GA concentration is not as significant as that of *mpk20-2*. These results are consistent with the differences observed between the *20-2* and *20-3* mutants in hypocotyl extension and root growth assays. My preliminary examination of the relationship between GA and these MPKs at least suggests that MPK20 may somehow be acting as a negative regulator in GA signaling pathways (Figure4.4). However further analysis is required to confirm this possibility. For instance, it might be informative to measure the hypocotyl elongation of *mpk20 ko* seedlings grown under a 16h/8h photo-period via microscope.

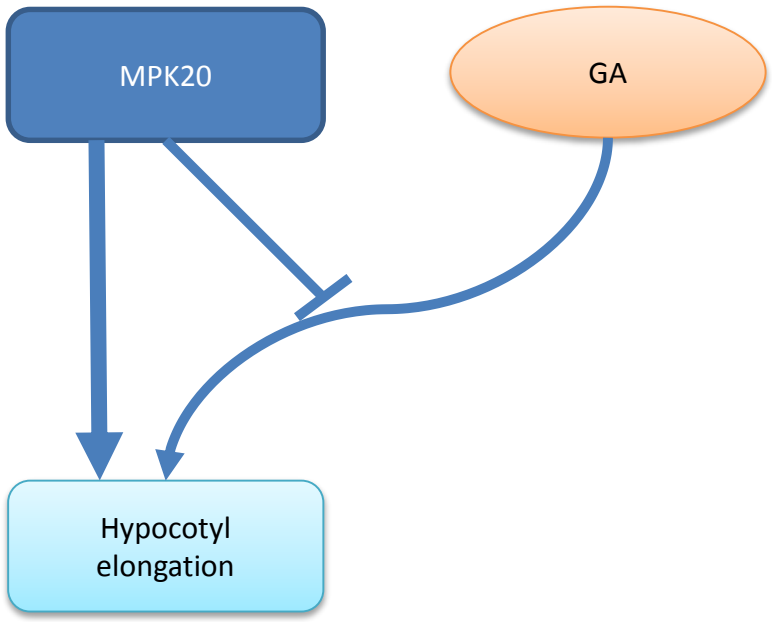


**Figure 4.4: The model shows that MPK20 normally promotes hypocotyl elongation, while negatively regulating a GA-related hypocotyl elongation pathway.**

## 4.3 The possible substrates of MPK20

Previous research has suggested that AtPIN1 may be a potential substrate of MPK20 (Frommer Group, www.associomics.org). As I did not succeed to purify the recombinant protein of MPK20, I was unable to establish whether or not AtPIN1 is a substrate of MPK20 via *in vitro* kinase assay. As another approach to identifying possible substrates of MPK20, we used an *in silico* kinase substrate prediction service from Kinexus [104]. Their prediction methodology is based on sequence databases in which they align 488 human protein kinase catalytic domain sequences with 10,000 known kinase-substrate phospho-site pairs. The amino acid sequence of the MPK20 catalytic domain was aligned with the PK database by using Kinexus' algorithms, which generated a frequency matrix of predicted phosphorylation-site amino acid sequences for potential MPK20 substrates. The most probable amino acid sequence around a MPK20 phosphorylation site is predicted to be: wwrdFPdSPyc(w)wt(w)yw. The capitalized residues have a high probability of being correctly predicted, while the lower case residues have a lower probability.

Some elements of this predicted sequence are not surprising since the MPK phosphorylation site motif is known to be -PXS/TP-. I next compared the sequence generated by this Kinexus prediction with the amino acid sequences of a number of candidate proteins, including not only AtPIN1, but also AtCesA1, AtCesA3, AtCesA6, MPK18, MPK19 and even MPK20, the last of which has been found to be capable of auto-phosphorylation [105]. This *in silico* analysis showed that all seven of these proteins have at least one peptide sequence that is very similar to the Kinexus-predicted MPK20 substrate peptide sequence (Figure 4.5). However, further protein-protein interaction experiments and protein phosphorylation analysis would be required to determine whether these predictions are meaningful.

| MPK20 peptide substrate | Amino acid group | | | | | | | | | | | | | | | |
|---|---|---|---|---|---|---|---|---|---|---|---|---|---|---|---|---|
| wwrdFPdSPyc(w)wt(w)yw | 1 | 1 | 4 | 3 | 1 | 1 | 3 | 2 | 1 | 2 | 2;1 | 1 | 2;1 | 2 | 1 | |
| | | | | | | | | | | | | | | | | |
| AtCESA1 | | | | | | | | | | | | | | | SCORE | |
| RFRRHRGSPRVEGDE | 4 | 1 | 4 | 4 | 4 | 4 | 1 | 2 | 1 | 4 | 1 | 3 | 1 | 3 | 3 | 6 |
| VEKRFGQSPVFIAAT | 1 | 3 | 4 | 4 | 1 | 1 | 2 | 2 | 1 | 1 | 1 | 1 | 1 | 1 | 2 | 9 |
| TVSGEIRTPDTQSVR | 2 | 1 | 2 | 1 | 3 | 1 | 4 | 2 | 1 | 3 | 2 | 2 | 2 | 1 | 4 | 6 |
| PIPSSRLTPYRVVII | 1 | 1 | 1 | 2 | 2 | 4 | 1 | 2 | 1 | 2 | 1 | 1 | 1 | 1 | 1 | 9 |
| GWTMQDGTPWPGNNT | 1 | 1 | 2 | 1 | 2 | 3 | 1 | 2 | 1 | 1 | 1 | 1 | 2 | 2 | 2 | 8 |
| LLGRQNRTPTIVIVW | 1 | 1 | 1 | 4 | 2 | 2 | 4 | 2 | 1 | 2 | 1 | 1 | 1 | 1 | 1 | 9 |
| SDRNAISSPYIDPRQ | 2 | 3 | 4 | 2 | 1 | 1 | 2 | 2 | 1 | 2 | 1 | 3 | 1 | 4 | 2 | 8 |
| | | | | | | | | | | | | | | | | |
| AtCESA3 | | | | | | | | | | | | | | | | |
| RYKRLKGSPAIPGDK | 4 | 2 | 4 | 4 | 1 | 4 | 1 | 2 | 1 | 1 | 1 | 1 | 1 | 3 | 4 | 7 |
| YSSDVNQSPNRRIVD | 2 | 2 | 2 | 3 | 1 | 2 | 2 | 2 | 1 | 2 | 4 | 4 | 1 | 1 | 3 | 6 |
| SGEFSAASPERLSVS | 2 | 1 | 3 | 1 | 2 | 1 | 1 | 2 | 1 | 3 | 4 | 1 | 2 | 1 | 2 | 6 |
| GWVMQDGTPWPGNNT | 1 | 1 | 1 | 1 | 2 | 3 | 1 | 2 | 1 | 1 | 1 | 1 | 2 | 2 | 2 | 8 |
| GGVPPSATPENLLKE | 1 | 1 | 1 | 1 | 1 | 2 | 1 | 2 | 1 | 3 | 2 | 1 | 1 | 4 | 1 | 9 |
| LMGRQNRTPTIVVVW | 1 | 1 | 1 | 4 | 2 | 2 | 4 | 2 | 1 | 2 | 1 | 1 | 1 | 1 | 1 | 9 |
| | | | | | | | | | | | | | | | | |
| AtCESA6 | | | | | | | | | | | | | | | | |
| GWRSVYCTPKLAAFK | 1 | 1 | 4 | 2 | 1 | 2 | 2 | 2 | 1 | 4 | 1 | 1 | 1 | 1 | 4 | 9 |
| GWTMQDGTPWPGNSV | 1 | 1 | 2 | 1 | 2 | 3 | 1 | 2 | 1 | 1 | 1 | 1 | 1 | 3 | 3 | 7 |
| RFKRLKGSPRVEGDE | 4 | 1 | 4 | 4 | 1 | 4 | 1 | 2 | 1 | 4 | 1 | 3 | 1 | 3 | 3 | 7 |
| EGKPSGLSPVDVFVS | 3 | 1 | 4 | 1 | 2 | 1 | 1 | 2 | 1 | 1 | 3 | 1 | 1 | 1 | 2 | 7 |
| GGMARNASPACLLKE | 1 | 1 | 1 | 1 | 4 | 2 | 1 | 2 | 1 | 1 | 2 | 1 | 1 | 4 | 3 | 7 |
| LEKKFGQSPVFVASA | 1 | 3 | 4 | 4 | 1 | 1 | 2 | 2 | 1 | 1 | 1 | 1 | 1 | 2 | 1 | 11 |

| MPK20 peptide substrate | Amino acid group | | | | | | | | | | | | | | | |
|---|---|---|---|---|---|---|---|---|---|---|---|---|---|---|---|---|
| wwrdFPdSPyc(w)wt(w)yw | 1 | 1 | 4 | 3 | 1 | 1 | 3 | 2 | 1 | 2 | 2;1 | 1 | 2;1 | 2 | 1 | |
| | | | | | | | | | | | | | | | | |
| AtMPK18 | | | | | | | | | | | | | | | | SCORE |
| ARVAFNDTPTTVFWT | 1 | 4 | 1 | 1 | 1 | 2 | 3 | 2 | 1 | 2 | 2 | 1 | 1 | 1 | 2 | 9 |
| GSFFSKYTPAIDVWS | 1 | 2 | 1 | 1 | 2 | 4 | 2 | 2 | 1 | 1 | 1 | 3 | 1 | 1 | 2 | 5 |
| LITDLLGTPKSETIS | 1 | 1 | 2 | 3 | 1 | 1 | 1 | 2 | 1 | 4 | 2 | 3 | 2 | 1 | 2 | 9 |
| FDPKDRPTPAEALAD | 1 | 3 | 1 | 4 | 3 | 4 | 1 | 2 | 1 | 1 | 3 | 1 | 1 | 1 | 3 | 5 |
| YFRSAVSSPHCYFRP | 2 | 1 | 4 | 2 | 1 | 1 | 2 | 2 | 1 | 4 | 2 | 2 | 1 | 4 | 1 | 9 |
| QNPVHQFSPTEPPAA | 2 | 2 | 1 | 1 | 4 | 2 | 1 | 2 | 1 | 2 | 3 | 1 | 1 | 1 | 1 | 6 |
| | | | | | | | | | | | | | | | | |
| AtMPK19 | | | | | | | | | | | | | | | | |
| ARVSFNDTPTTVFWT | 1 | 4 | 1 | 1 | 2 | 2 | 3 | 2 | 1 | 2 | 2 | 1 | 1 | 1 | 2 | 8 |
| GSFCSKYTPAIDIWS | 1 | 2 | 1 | 2 | 2 | 4 | 2 | 2 | 1 | 1 | 1 | 3 | 1 | 1 | 2 | 5 |
| LITDLLGTPKSETIA | 1 | 1 | 2 | 3 | 1 | 1 | 1 | 2 | 1 | 4 | 2 | 3 | 2 | 1 | 1 | 10 |
| VLPPQTISPNCFFHP | 1 | 1 | 1 | 1 | 2 | 2 | 1 | 2 | 1 | 2 | 2 | 1 | 1 | 4 | 1 | 9 |
| | | | | | | | | | | | | | | | | |
| AtMPK20 | | | | | | | | | | | | | | | | |
| ARVAFNDTPTTIFWT | 1 | 4 | 1 | 1 | 1 | 2 | 3 | 2 | 1 | 2 | 2 | 1 | 1 | 1 | 2 | 9 |
| LMTDLLGTPSLDTIS | 1 | 1 | 2 | 3 | 1 | 1 | 1 | 2 | 1 | 2 | 1 | 3 | 2 | 1 | 2 | 10 |
| GSFYSKYTPAIDIWS | 1 | 2 | 1 | 2 | 2 | 4 | 2 | 2 | 1 | 1 | 1 | 3 | 1 | 1 | 2 | 5 |
| | | | | | | | | | | | | | | | | |
| AtPIN1 | | | | | | | | | | | | | | | | |
| VKWWKIFTPDQCSGI | 1 | 4 | 1 | 1 | 4 | 1 | 1 | 2 | 1 | 3 | 2 | 2 | 2 | 1 | 1 | 7 |
| RSQGLSATPRPSNLT | 4 | 2 | 2 | 1 | 1 | 2 | 1 | 2 | 1 | 4 | 1 | 2 | 2 | 1 | 2 | 5 |
| LQSSRNPTPRGSSFN | 1 | 2 | 2 | 2 | 4 | 2 | 1 | 2 | 1 | 4 | 1 | 4 | 4 | 1 | 2 | 4 |
| VFGSKGPTPRPSNYE | 1 | 1 | 1 | 2 | 4 | 1 | 1 | 2 | 1 | 4 | 1 | 2 | 2 | 2 | 3 | 8 |
| APNPGMFSPNTGGGG | 1 | 1 | 2 | 1 | 1 | 1 | 1 | 2 | 1 | 2 | 2 | 1 | 1 | 1 | 1 | 11 |
| FVWSSSASPVSDVFG | 1 | 1 | 1 | 2 | 2 | 2 | 1 | 2 | 1 | 1 | 2 | 3 | 1 | 1 | 1 | 7 |

**Figure 4.5: Analysis of the peptide sequence in potential substrates of MPK20**

In "Amino acid group" row, "1" represents nonpolar side-chain amino acids, "2" represents polar side-chain amino acids, "3" represents electrically charged side-chain (acidic) amino acids, and "4" represents electrically charged side-chains (basic) amino acids. The "score" rows show the number of amino acids that belong to the same group as the Kinexus-predicted MPK20 peptide substrate (positive matches are highlighted in yellow in the figure).

## 4.4 Conclusions

The work in this thesis mainly focuses on the examination of possible biological functions of a Group D MAPK, MPK20, in Arabidopsis seedlings. The results indicate that MPK20 probably plays a role in hypocotyl and root growth, and may be also involved in GA-mediated growth. To try to gain a better understanding of MPK20's functions, the *mpk20 ko* mutant was examined with or without the presence of the close paralogues of MPK20, namely, -- MPK18 and MPK19. Intricate interactions between these three MPKs were observed, which do not seem to be explained by any simple relationship model. The results are consistent with a close but not identical functional relationship between MPK20 and its two paralogues, MPK18 and MPK19.

Further work is required in order to confirm the conjectures proposed in this chapter, and to pinpoint the redundant, as well as the unique, parts of the each of these Group D MPKs' functions.

## References:


1. Persson, S., et al., *Identification of genes required for cellulose synthesis by regression analysis of public microarray data sets.* Proc Natl Acad Sci U S A, 2005. **102**(24): p. 8633-8.
2. Hunter, T., *A thousand and one protein kinases.* Cell, 1987. **50**(6): p. 823-829.
3. Rubin, G.M., et al., *Comparative genomics of the eukaryotes.* Science, 2000. **287**(5461): p. 2204-2215.
4. Lander, E.S., et al., *Initial sequencing and analysis of the human genome.* Nature, 2001. **409**(6822): p. 860-921.
5. Swain, P.K., et al., *Multiple phosphorylated isoforms of nrl are expressed in rod photoreceptors.* Journal of Biological Chemistry, 2001. **276**(39): p. 36824-36830.
6. Sturgill, T.W. and L.B. Ray, *Muscle proteins related to microtubule associated protein-2 are substrates for an insulin-stimulatable kinase.* Biochemical and Biophysical Research Communications, 1986. **134**(2): p. 565-571.
7. Ichimura, K., et al., *Mitogen-activated protein kinase cascades in plants: A new nomenclature.* Trends in plant science, 2002. **7**(7): p. 301-308.
8. Kovtun, Y., et al., *Functional analysis of oxidative stress-activated mitogen-activated protein kinase cascade in plants.* Proceedings of the National Academy of Sciences of the United States of America, 2000. **97**(6): p. 2940-2945.
9. Mizoguchi, T., et al., *A gene encoding a mitogen-activated protein kinase kinase kinase is induced simultaneously with genes for a mitogen-activated protein kinase and an s6 ribosomal protein kinase by touch, cold, and water stress in arabidopsis thaliana.* Proceedings of the National Academy of Sciences of the United States of America, 1996. **93**(2): p. 765-769.
10. Kieber, J.J., et al., *Ctr1, a negative regulator of the ethylene response pathway in arabidopsis, encodes a member of the raf family of protein-kinases.* Cell, 1993. **72**(3): p. 427-441.
11. Nakagami, H., et al., *A mitogen-activated protein kinase kinase kinase mediates reactive oxygen species homeostasis in arabidopsis.* Journal of Biological Chemistry, 2006. **281**(50): p. 38697-38704.
12. Ichimura, K., et al., *Isolation of atmekk1 (a map kinase kinase kinase) - interacting proteins and analysis of a map kinase cascade in arabidopsis.* Biochemical and Biophysical Research Communications, 1998. **253**(2): p. 532-543.
13. Kong, Q., et al., *The mekk1-mkk1/mkk2-mpk4 kinase cascade negatively regulates immunity mediated by a mitogen-activated protein kinase kinase kinase in arabidopsis.* Plant Cell, 2012. **24**(5): p. 2225-2236.
14. Gao, M., et al., *Mekk1, mkk1/mkk2 and mpk4 function together in a mitogen-activated protein kinase cascade to regulate innate immunity in plants.* Cell research, 2008. **18**(12): p. 1190-1198.

15. Xing, Y., W. Jia, and J. Zhang, *Atmkk1 mediates aba‐induced cat1 expression and h2o2 production via atmpk6‐coupled signaling in arabidopsis.* The Plant Journal, 2008. **54**(3): p. 440-451.

16. Teige, M., et al., *The mkk2 pathway mediates cold and salt stress signaling in arabidopsis.* Molecular cell, 2004. **15**(1): p. 141-152.

17. Asai, T., et al., *Map kinase signalling cascade in arabidopsis innate immunity.* Nature, 2002. **415**(6875): p. 977-983.

18. Kim, S.-H., et al., *Arabidopsis mkk4 mediates osmotic-stress response via its regulation of mpk3 activity.* Biochemical and biophysical research communications, 2011. **412**(1): p. 150-154.

19. Dai, Y., et al., *Increased expression of map kinase kinase7 causes deficiency in polar auxin transport and leads to plant architectural abnormality in arabidopsis.* The Plant Cell Online, 2006. **18**(2): p. 308-320.

20. Xu, J., et al., *Activation of MAPK kinase 9 induces ethylene and camalexin biosynthesis and enhances sensitivity to salt stress in Arabidopsis.* Journal of Biological Chemistry, 2008. **283**(40): p. 26996-27006.

21. Knighton, D.R., et al., *Crystal structure of the catalytic subunit of cyclic adenosine monophosphate-dependent protein kinase.* Science, 1991. **253**(5018): p. 407-414.

22. Arnold, K., et al., *The Swiss-model workspace: A web-based environment for protein structure homology modelling.* Bioinformatics, 2006. **22**(2): p. 195-201.

23. Biasini, M., et al., *Swiss-model: Modelling protein tertiary and quaternary structure using evolutionary information.* Nucleic Acids Research, 2014. **42**(W1): p. W252-W258.

24. Kiefer, F., et al., *The Swiss-model repository and associated resources.* Nucleic Acids Research, 2009. **37**: p. D387-D392.

25. Guex, N., M.C. Peitsch, and T. Schwede, *Automated comparative protein structure modeling with Swiss-model and Swiss-pdbviewer: A historical perspective.* Electrophoresis, 2009. **30**: p. S162-S173.

26. Cargnello, M. and P.P. Roux, *Activation and function of the MAPKs and their substrates, the MAPK-activated protein kinases (vol 75, pg 50, 2011).* Microbiology and Molecular Biology Reviews, 2012. **76**(2): p. 496-496.

27. Lampard, G.R., C.A. MacAlister, and D.C. Bergmann, *Arabidopsis stomatal initiation is controlled by MAPK-mediated regulation of the bhlh speechless.* Science, 2008. **322**(5904): p. 1113-1116.

28. Lampard, G.R., et al., *Novel and expanded roles for MAPK signaling in Arabidopsis stomatal cell fate revealed by cell type-specific manipulations.* Plant Cell, 2009. **21**(11): p. 3506-3517.

29. Liu, Y.D. and S.Q. Zhang, *Phosphorylation of 1-aminocyclopropane-1-carboxylic acid synthase by MPK6, a stress-responsive mitogen-activated protein kinase, induces ethylene biosynthesis in Arabidopsis.* Plant Cell, 2004. **16**(12): p. 3386-3399.

30. Kim, T.W., et al., *Brassinosteroid regulates stomatal development by GSK3-mediated inhibition of a MAPK pathway.* Nature, 2012. **482**(7385): p. 419-U1526.

31. Ren, D.T., et al., *A fungal-responsive MAPK cascade regulates phytoalexin biosynthesis in arabidopsis.* Proceedings of the National Academy of Sciences of the United States of America, 2008. **105**(14): p. 5638-5643.

32. Samuel, M.A., et al., *Overexpression of SIPK in tobacco enhances ozone-induced ethylene formation and blocks ozone-induced SA accumulation.* Journal of Experimental Botany, 2005. **56**(418): p. 2195-2201.

33. Yoo, S.D., et al., *Dual control of nuclear EIN3 by bifurcate MAPK cascades in C2H4 signalling.* Nature, 2008. **451**(7180): p. 789-U1.

34. Zhang, S.Q. and D.F. Klessig, *Resistance gene N-mediated de novo synthesis and activation of a tobacco mitogen-activated protein kinase by tobacco mosaic virus infection.* Proceedings of the National Academy of Sciences of the United States of America, 1998. **95**(13): p. 7433-7438.

35. Ichimura, K., et al., *Various abiotic stresses rapidly activate Arabidopsis map kinases AtMPK4 and AtMPK6.* Plant J, 2000. **24**(5): p. 655-65.

36. Stanko, V., et al., *Timing is everything: Highly specific and transient expression of a map kinase determines auxin-induced leaf venation patterns in Arabidopsis.* Mol Plant, 2014. **7**(11): p. 1637-52.

37. Ulm, R., et al., *Distinct regulation of salinity and genotoxic stress responses by Arabidopsis MAP kinase phosphatase 1.* EMBO J, 2002. **21**(23): p. 6483-93.

38. Droillard, M.J., et al., *Involvement of MPK4 in osmotic stress response pathways in cell suspensions and plantlets of Arabidopsis thaliana: Activation by hypoosmolarity and negative role in hyperosmolarity tolerance.* FEBS Lett, 2004. **574**(1-3): p. 42-8.

39. Ichimura, K., et al., *MEKK1 is required for MPK4 activation and regulates tissue-specific and temperature-dependent cell death in Arabidopsis.* J Biol Chem, 2006. **281**(48): p. 36969-76.

40. Furuya, T., D. Matsuoka, and T. Nanmori, *Membrane rigidification functions upstream of the MEKK1-MKK2-MPK4 cascade during cold acclimation in Arabidopsis thaliana.* FEBS Lett, 2014. **588**(11): p. 2025-30.

41. Wang, F., W. Jing, and W. Zhang, *The mitogen-activated protein kinase cascade MKK1-MPK4 mediates salt signaling in rice.* Plant Sci, 2014. **227**: p. 181-9.

42. Zeng, Q.N., J.G. Chen, and B.E. Ellis, *AtMPK4 is required for male-specific meiotic cytokinesis in Arabidopsis.* Plant Journal, 2011. **67**(5): p. 895-906.

43. Kosetsu, K., et al., *The map kinase MPK4 is required for cytokinesis in Arabidopsis thaliana.* Plant Cell, 2010. **22**(11): p. 3778-90.

44. Takahashi, Y., et al., *Hinkel kinesin,ANP MAPKKKs and MKK6/ANQ MAPKK, which phosphorylates and activates MPK4 MAPK, constitute a pathway that is required for cytokinesis in Arabidopsis thaliana.* Plant Cell Physiol, 2010. **51**(10): p. 1766-76.

45. Schweighofer, A., et al., *The PP2c-type phosphatase AP2c1, which negatively regulates MPK4 and MPK6, modulates innate immunity, jasmonic acid, and ethylene levels in Arabidopsis.* Plant Cell, 2007. **19**(7): p. 2213-24.

46. Suarez-Rodriguez, M.C., et al., *MEKK1 is required for flg22-induced MPK4 activation in Arabidopsis plants.* Plant Physiol, 2007. **143**(2): p. 661-9.

47. Pitzschke, A., et al., *A major role of the MEKK1-MKK1/2-MPK4 pathway in ROS signalling.* Mol Plant, 2009. **2**(1): p. 120-37.

48. Lee, J.S., et al., *Comprehensive analysis of protein-protein interactions between Arabidopsis MAPKs and MAPK kinases helps define potential MAPK signalling modules.* Plant Signal Behav, 2008. **3**(12): p. 1037-41.

49. Eschen-Lippold, L., et al., *MPK11-a fourth elicitor-responsive mitogen-activated protein kinase in Arabidopsis thaliana.* Plant Signal Behav, 2012. **7**(9): p. 1203-5.

50. Jammes, F., et al., *MAP kinases MPK9 and MPK12 are preferentially expressed in guard cells and positively regulate ROS-mediated ABA signaling.* Proc Natl Acad Sci U S A, 2009. **106**(48): p. 20520-5.

51. Des Marais, D.L., et al., *Variation in MPK12 affects water use efficiency in Arabidopsis and reveals a pleiotropic link between guard cell size and ABA response.* Proc Natl Acad Sci U S A, 2014. **111**(7): p. 2836-41.

52. Mao, P., et al., *WRKY62 transcription factor acts downstream of cytosolic NPR1 and negatively regulates jasmonate-responsive gene expression.* Plant Cell Physiol, 2007. **48**(6): p. 833-42.

53. Popescu, S.C., et al., *MAPK target networks in Arabidopsis thaliana revealed using functional protein microarrays.* Genes Dev, 2009. **23**(1): p. 80-92.

54. Hua, Z.M., X. Yang, and M.E. Fromm, *Activation of the NaCl- and drought-induced rRD29a and RD29b promoters by constitutively active Arabidopsis MAPKK or MAPK proteins.* Plant Cell Environ, 2006. **29**(9): p. 1761-70.

55. Shi, J., et al., *GhMPK7, a novel multiple stress-responsive cotton groupC MAPK gene, has a role in broad spectrum disease resistance and plant development.* Plant Mol Biol, 2010. **74**(1-2): p. 1-17.

56. He, C.Z., et al., *BWMK1,a novel MAP kinase induced by fungal infection and mechanical wounding in rice.* Molecular Plant-Microbe Interactions, 1999. **12**(12): p. 1064-1073.

57. Agrawal, G.K., et al., *Novel rice MAP kinases OsMSRMK3 and OsWJUMK1 involved in encountering diverse environmental stresses and developmental regulation.* Biochemical and Biophysical Research Communications, 2003. **300**(3): p. 775-783.

58. Reyna, N.S. and Y.N. Yang, *Molecular analysis of the rice MAP kinase gene family in relation to Magnaporthe grisea infection.* Molecular Plant-Microbe Interactions, 2006. **19**(5): p. 530-540.

59. Schoenbeck, M.A., et al., *The alfalfa (Medicago sativa) TDY1 gene encodes a mitogen-activated protein kinase homolog.* Molecular Plant-Microbe Interactions, 1999. **12**(10): p. 882-893.

60. Soyano, T., et al., *NQK1/NtMEK1 is a MAPKK that acts in the NPK1 MAPKKK-mediated MAPK cascade and is required for plant cytokinesis.* Genes & Development, 2003. **17**(8): p. 1055-1067.

61. Pan, J.W., et al., *ZmMPK17, a novel maize group D MAP kinase gene, is involved in multiple stress responses.* Planta, 2012. **235**(4): p. 661-676.

62. Persson, S., et al., *Identification of genes required for cellulose synthesis by regression analysis of public microarray data sets.* Proceedings of the National Academy of Sciences of the United States of America, 2005. **102**(24): p. 8633-8638.

63. Nuhse, T.S., et al., *Phosphoproteomics of the Arabidopsis plasma membrane and a new phosphorylation site database.* Plant Cell, 2004. **16**(9): p. 2394-405.

64. Michniewicz, M., et al., *Antagonistic regulation of PIN phosphorylation by PP2a and PINOID directs auxin flux.* Cell, 2007. **130**(6): p. 1044-1056.

65. Lalonde, S., et al., *Molecular and cellular approaches for the detection of protein–protein interactions: Latest techniques and current limitations.* The Plant Journal, 2008. **53**(4): p. 610-635.

66. Hamel, L.-P., et al., *Ancient signals: Comparative genomics of plant MAPK and MAPKK gene families.* Trends in plant science, 2006. **11**(4): p. 192-198.

67. Shen, H., et al., *OsWRKY30 is activated by MAP kinases to confer drought tolerance in rice.* Plant molecular biology, 2012. **80**(3): p. 241-253.

68. Walia, A., et al., *Arabidopsis mitogen-activated protein kinase MPK18 mediates cortical microtubule functions in plant cells.* Plant Journal, 2009. **59**(4): p. 565-575.

69. Fujita, S., et al., *An atypical tubulin kinase mediates stress-induced microtubule depolymerization in Arabidopsis.* Current Biology, 2013. **23**(20): p. 1969-1978.

70. Cassimeris, L., et al., *Lewin's cells*. 2011: Jones & Bartlett Learning.

71. Wightman, R. and S. Turner, *Trafficking of the plant cellulose synthase complex.* Plant Physiol, 2010. **153**(2): p. 427-32.

72. Mueller, S.C. and R.M. Brown, Jr., *Evidence for an intramembrane component associated with a cellulose microfibril-synthesizing complex in higher plants.* J Cell Biol, 1980. **84**(2): p. 315-26.

73. Herth, W., *Plasma-membrane rosettes involved in localized wall thickening during xylem vessel formation of Lepidium sativum l.* Planta, 1985. **164**(1): p. 12-21.

74. Desprez, T., et al., *Organization of cellulose synthase complexes involved in primary cell wall synthesis in Arabidopsis thaliana.* Proc Natl Acad Sci U S A, 2007. **104**(39): p. 15572-7.

75. Persson, S., et al., *Genetic evidence for three unique components in primary cell-wall cellulose synthase complexes in Arabidopsis.* Proc Natl Acad Sci U S A, 2007. **104**(39): p. 15566-71.

76. Fagard, M., et al., *PROCUSTE1 encodes a cellulose synthase required for normal cell elongation specifically in roots and dark-grown hypocotyls of Arabidopsis.* Plant Cell, 2000. **12**(12): p. 2409-2424.

77. Obayashi, T., et al., *ATTED-II provides coexpressed gene networks for Arabidopsis.* Nucleic Acids Res, 2009. **37**(Database issue): p. D987-91.

78. Obayashi, T., et al., *ATTED-II updates: Condition-specific gene coexpression to extend coexpression analyses and applications to a broad range of flowering plants.* Plant Cell Physiol, 2011. **52**(2): p. 213-9.

79. Obayashi, T. and K. Kinoshita, *Coexpression landscape in ATTED-II: Usage of gene list and gene network for various types of pathways.* Journal of Plant Research, 2010. **123**(3): p. 311-319.

80. Winter, D., et al., *An "electronic fluorescent pictograph" browser for exploring and analyzing large-scale biological data sets.* Plos One, 2007. **2**(8).

81. Ye, G.N., et al., *Arabidopsis ovule is the target for Agrobacterium in planta vacuum infiltration transformation.* The plant journal, 1999. **19**(3): p. 249-257.

82. Finch-Savage, W.E. and G. Leubner-Metzger, *Seed dormancy and the control of germination.* New Phytologist, 2006. **171**(3): p. 501-523.

83. Lu, G., et al., *Identification of OsbZIP72 as a positive regulator of ABA response and drought tolerance in rice.* Planta, 2009. **229**(3): p. 605-615.

84. Brock, A.K., et al., *The Arabidopsis mitogen-activated protein kinase phosphatase PP2c5 affects seed germination, stomatal aperture, and abscisic acid-inducible gene expression.* Plant Physiol, 2010. **153**(3): p. 1098-111.

85. Gendreau, E., et al., *Cellular basis of hypocotyl growth in Arabidopsis thaliana.* Plant Physiol, 1997. **114**(1): p. 295-305.

86. Cowling, R.J., et al., *Gibberellin dose-response regulation of GA4 gene transcript levels in Arabidopsis.* Plant Physiol, 1998. **117**(4): p. 1195-203.

87. Cowling, R.J. and N.P. Harberd, *Gibberellins control Arabidopsis hypocotyl growth via regulation of cellular elongation.* Journal of Experimental Botany, 1999. **50**(337): p. 1351-1357.

88. Raz, V. and M. Koornneef, *Cell division activity during apical hook development.* Plant Physiology, 2001. **125**(1): p. 219-226.

89. Schneider, C.A., W.S. Rasband, and K.W. Eliceiri, *NIH image to ImageJ: 25 years of image analysis.* Nat Methods, 2012. **9**(7): p. 671-5.

90. Overvoorde, P., H. Fukaki, and T. Beeckman, *Auxin control of root development.* Cold Spring Harb Perspect Biol, 2010. **2**(6): p. a001537.

91. Luschnig, C., et al., *EIR1, a root-specific protein involved in auxin transport, is required for gravitropism in Arabidopsis thaliana.* Genes & Development, 1998. **12**(14): p. 2175-2187.

92. Ljung, K., R.P. Bhalerao, and G. Sandberg, *Sites and homeostatic control of auxin biosynthesis in Arabidopsis during vegetative growth.* Plant J, 2001. **28**(4): p. 465-74.

93. Mansfield, S.G. and L.G. Briarty, *The dynamics of seedling and cotyledon cell development in Arabidopsis thaliana during reserve mobilization.* International Journal of Plant Sciences, 1996. **157**(3): p. 280-295.

94. Raghavan, V., *Role of 2,4-dichlorophenoxyacetic acid (2,4-d) in somatic embryogenesis on cultured zygotic embryos of Arabidopsis: Cell expansion, cell cycling, and morphogenesis during continuous exposure of embryos to 2,4-D.* American Journal of Botany, 2004. **91**(11): p. 1743-1756.

95. Ludwig, A.A., et al., *Ethylene-mediated cross-talk between calcium-dependent protein kinase and MAPK signaling controls stress responses in plants.* Proceedings of the National Academy of Sciences of the United States of America, 2005. **102**(30): p. 10736-10741.

96. Zhang, T., et al., *Diverse signals converge at MAPK cascades in plant.* Plant Physiology and Biochemistry, 2006. **44**(5-6): p. 274-283.

97. De Grauwe, L., J. Dugardeyn, and D. Van Der Straeten, *Novel mechanisms of ethylene-gibberellin crosstalk revealed by the GAI ETO2-1 double mutant.* Plant Signal Behav, 2008. **3**(12): p. 1113-5.

98. Bradford, K.J. and S.F. Yang, *Xylem transport of 1-aminocyclopropane-1-carboxylic acid, an ethylene precursor, in waterlogged tomato plants.* Plant Physiology, 1980. **65**(2): p. 322-326.

99. Bleecker, A.B., et al., *Insensitivity to ethylene conferred by a dominant mutation in Arabidopsis thaliana.* Science, 1988. **241**(4869): p. 1086-9.

100. Larsen, P.B. and C. Chang, *The Arabidopsis EER1 mutant has enhanced ethylene responses in the hypocotyl and stem.* Plant Physiology, 2001. **125**(2): p. 1061-1073.

101. Nagata, N., et al., *Treatment of dark-grown Arabidopsis thaliana with a brassinosteroid-biosynthesis inhibitor, brassinazole, induces some characteristics of light-grown plants.* Planta, 2000. **211**(6): p. 781-790.

102. Fu, X.D. and N.P. Harberd, *Auxin promotes Arabidopsis root growth by modulating gibberellin response.* Nature, 2003. **421**(6924): p. 740-743.

103. Brandao, M.M., L.L. Dantas, and M.C. Silva-Filho, *AtPIN: Arabidopsis thaliana protein interaction network.* BMC Bioinformatics, 2009. **10**: p. 454.

104. Safaei, J., et al., *Prediction of 492 human protein kinase substrate specificities.* Proteome Sci, 2011. **9 Suppl 1**: p. S6.

105. Nemoto, K., et al., *Autophosphorylation profiling of Arabidopsis protein kinases using the cell-free system.* Phytochemistry, 2011. **72**(10): p. 1136-44.

106. Higgins, D.G. and P.M. Sharp, *Fast and sensitive multiple sequence alignments on a microcomputer.* Comput Appl Biosci, 1989. **5**(2): p. 151-3.

107. Thompson, J.D., F. Plewniak, and O. Poch, *Balibase: A benchmark alignment database for the evaluation of multiple alignment programs.* Bioinformatics, 1999. **15**(1): p. 87-8.

108. Notredame, C., D.G. Higgins, and J. Heringa, *T-coffee: A novel method for fast and accurate multiple sequence alignment.* J Mol Biol, 2000. **302**(1): p. 205-17.

109. Katoh, K., et al., *Mafft: A novel method for rapid multiple sequence alignment based on fast fourier transform.* Nucleic Acids Res, 2002. **30**(14): p. 3059-66.

110. Edgar, R.C., *Muscle: Multiple sequence alignment with high accuracy and high throughput.* Nucleic Acids Res, 2004. **32**(5): p. 1792-7.

# Appendix

1. Protein sequences alignment by using Clustal X

By the late 1990s, Clustal X was already able to sufficiently align medium-sized data sets. The alignment results are high quantity and do not need to be edited manually very often[106]. Later, by the appearance of BALiBASE (the first custom made benchmark test set) and T-Coffee code, it is possible to accurately make alignments of very divergent proteins [107, 108]. Due to the increasing computer speeds and the appearance of MAFFT (Multiple Alignment using Fast Fourier Transform) and MUSCLE (Multiple Sequence Comparison by Log-Expectation), the alignment process has become extremely fast and it is possible to conduct alignments of thousands of sequences [109, 110]. Now, by using the newest version of Clustal X, the alignment of larger data sets is allowed, the speed of aligning is increased, and the accuracy of the alignment is increased.